AD-A184 822 FUNDAMENTAL STUDIES IN THE OM-CVD GROWTH OF GA-IN-AS-SB 1/1
(U) NORTH CAROLINA STATE UNIV AT RALEIGH DEPT OF
ELECTRICAL AND C S M BEDAIR ET AL MAY 87
UNCLASSIFIED ARO-19788 10-MS DAAG29-83-K-0118 F/G 11/3 NL

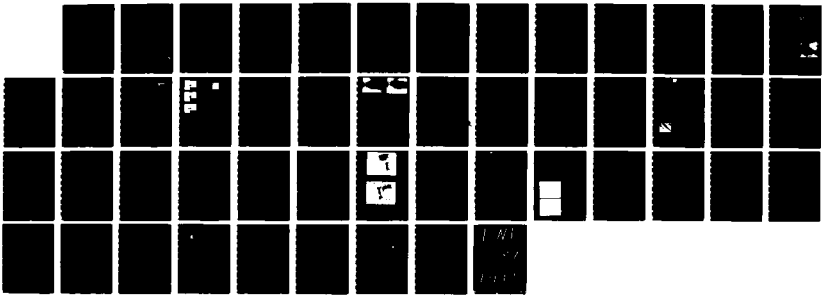

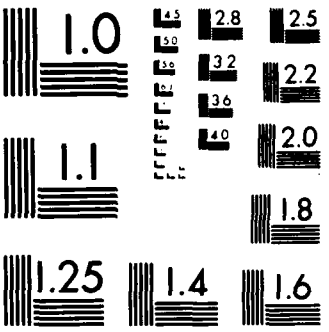

UNCLASSIFIED
SECURITY CLASSIFICATION OF THIS PAGE

(2)

DTIC FILE COPY

REPORT DOCUMENTATION PAGE

1a. REPORT SECURITY CLASSIFICATION	1b. RESTRICTIVE MARKINGS
AD-A184 822	3 DISTRIBUTION/AVAILABILITY OF REPORT Approved for public release; distribution unlimited.
	5. MONITORING ORGANIZATION REPORT NUMBER(S) ARO 19788.10-MS
6a. NAME OF PERFORMING ORGANIZATION Elec. & Comp. Engr. Dept. N. C. State University	6b. OFFICE SYMBOL (If applicable)
6c. ADDRESS (City, State, and ZIP Code) Box 7911 Raleigh, North Carolina 27695-7911	7a. NAME OF MONITORING ORGANIZATION U. S. Army Research Office 7b. ADDRESS (City, State, and ZIP Code) P. O. Box 12211 Research Triangle Park, NC 27709-2211
8a. NAME OF FUNDING/SPONSORING ORGANIZATION U. S. Army Research Office	8b. OFFICE SYMBOL (If applicable)
8c. ADDRESS (City, State, and ZIP Code) P. O. Box 12211 Research Triangle Park, NC 27709-2211	9. PROCUREMENT INSTRUMENT IDENTIFICATION NUMBER DAAG29-83-K-0118 10. SOURCE OF FUNDING NUMBERS

PROGRAM ELEMENT NO.	PROJECT NO.	TASK NO.	WORK UNIT ACCESSION NO.

11. TITLE (Include Security Classification)
Fundamental Studies of the OM-CVD Growth of Ga-In-As-Sb

12 PERSONAL AUTHOR(S)
S. M. Bedair and J. R. Hauser

13a. TYPE OF REPORT	13b. TIME COVERED	14. DATE OF REPORT (Year, Month, Day)	15. PAGE COUNT
Final	FROM 9/1/83 TO 2/28/87	May 1987	9+

16. SUPPLEMENTARY NOTATION
The view, opinions and/or findings contained in this report are those of the author(s) and should not be construed as an official Department of the Army position policy, or decision, unless so designated by other documentation.

17 COSATI CODES		
FIELD	GROUP	SUB-GROUP

18. SUBJECT TERMS (Continue on reverse if necessary and identify by block number)

19 ABSTRACT (Continue on reverse if necessary and identify by block number)

We have studied the fundamental OM-CVD growth processes. Several ternary and quaternary alloys have been synthesized and their structural, optical and electrical properties were studied. We have developed Atomic Layer Epitaxy to control the deposition process to the atomic level. Strained layer superlattices have been used as buffer layers to reduce defects originating from GaAs substrates.

20 DISTRIBUTION/AVAILABILITY OF ABSTRACT	21. ABSTRACT SECURITY CLASSIFICATION
☐ UNCLASSIFIED/UNLIMITED ☐ SAME AS RPT. ☐ DTIC USERS	Unclassified
22a. NAME OF RESPONSIBLE INDIVIDUAL	22b. TELEPHONE (Include Area Code) / 22c. OFFICE SYMBOL

DD FORM 1473, 84 MAR 83 APR edition may be used until exhausted. All other editions are obsolete.

SECURITY CLASSIFICATION OF THIS PAGE
UNCLASSIFIED

ARO 19788.10-MS

FUNDAMENTAL STUDIES IN THE OM-CVD GROWTH OF Ga-In-As-Sb

Final Report

S. M. Bedair and J. R. Hauser

May 1987

U.S. Army Research Office

DAAG29-83-K-0118

Electrical and Computer Engineering Department
North Carolina State University
Raleigh, North Carolina 27695-7911

Several research activities were conducted during the last three years. They are mainly along the following directions.

A) GROWTH AND CHARACTERIZATION OF InAsSb FOR LONG WAVELENGTH DETECTORS

1) OM-CVD Growth of InAsSb

OM-CVD growth of InSb and $InAs_{1-x}Sb_x$ has been obtained using triethylindium (TEI), trimethylantimony (TMS) and arsine (AsH_3) on (100)GaAs, (100)InSb and (111)-B InSb substrates. InSb with excellent morphology was achieved on both (100)InSb and (111)-B substrates. The measured electron mobility at 300°K of undoped InSb grown on (100)GaAs semi-insulating substrates was 40,000 $cm^2/V-sec$ at a carrier concentration of 2.0×10^{16} cm^{-3}. $InAs_{1-x}Sb_x$ ($0.0 \leq x \leq 0.75$) with mirror-like surfaces have been grown on InSb and InAs substrates. This may be the first successful epitaxial growth of high quality layers of this ternary in the composition range $0.5 \leq x \leq 0.7$, having the lowest bandgap, $Eg \simeq 0.1$ eV that can be achieved in the III-V compounds. Solid composition variations as a function of growth temperature and InSb substrate orientation have also been studies.

2) Fabrication of Infrared Detectors in III-V Compounds That Can Cover Part of the 8-12 μm Spectral

P-n junctions have been fabricated in InSb and $InAs_{1-x}Sb_x$ ($0.4 < x < 0.7$) using OM-CVD. These junctions showed soft breakdown in addition to forward characteristics with a diode factor greater than 2. The ternary alloy has a cutoff wavelength in the 9-11 μm range, thus providing a potential material system for detectors covering part of the 8-12 μm range.

3) Growth of Epitaxial Layers Based on In-As-Sb-Bi Material System for Infrared Detectors

InBi is a semimetal, thus, one approach to reduce the bandgap of InSb or InAsSb is to add Bi, to form InSbBi and InAsSbBi ternary and quaternary compounds, respectively. $InAs_{0.4}Sb_{0.6}$ detectors built in our laboratory have a cutoff wavelength of about 11 μm. This cut-off wavelength can be extended to longer wavelength by adding Bi to cover the 8-14 μm spectral range. This material system may offer a real alternative to HgCdTe. The problem of the Bi compound is its limited solid solubility, 2.2% in InSb, and maybe even lower in InAsSb. We have grown films of InAsBi, InSbBi and InAsSbBi by OM-CVD on InSb and GaAs substrates and we are in the process of characterizing these films by optical and electrical techniques.

4) Growth of $InAs_{1-x}Sb_x$ ($0 < x < 1$) and InSb-InAsSb Superlattices by Molecular Beam Epitaxy

Thin films of $InAs_{1-x}Sb_x$ ($0 < x < 1$) have been deposited on GaAs and InSb substrates in the temperature range 300-400°C using molecular beam epitaxy. The solid composition was found to be quite sensitive to the Sb flux and less sensitive to the As flux. InSb-InAsSb superlattice structures have also been grown and studied. Both the ternary alloy and the superlattice structures can be potential material systems for detectors covering the 8-12 μ range.

B) STRAINED LAYER SUPERLATTICES

1) Defects Reduction in Epitaxial Growth Using Superlattice Buffer Layers

GaAsP-InGaAs strained-layer superlattices grown lattice-matched to GaAs have been used to reduce the density of threading dislocations originating from the GaAs substrate. GaAs epitaxial layers grown on the GaAsP-InGaAs superlattice buffer layers showed a dislocation density lower by at least an order of magnitude than that obtained from epitaxial layers grown directly on GaAs substrates. Transmission electron microscopy showed that dislocations originating from the GaAs substrate do not penetrate the GaAsP-InGaAs superlattice layers. We expect that such results will have a great impact on GaAs IC technology.

2) GaAsP-GaInAsSb Strained Layered Superlattices

OM-CVD has been used to grow $GaAs_{1-z}P_z - Ga_{1-x}In_xAs$, $GaAs_{1-z}P_z - GaAs_{1-y}Sb_y$ and $GaAs_{1-z}P_z - Ga_{1-x}In_xAs_{1-y}Sb_y$ superlattices in the composition range $0 \leq x \leq 0.25$, $0 \leq y \leq 0.3$ and $0 \leq z \leq 0.5$. Growth parameters for the synthesis of these new structures have been determined. SL structures are characterized by x-ray diffraction, photoluminescence and electron microprobe. Light-emitting diodes (LED's), based on this superlattices have been fabricated. This new structure can be grown lattice matched to GaAs substrates and thus has potential applications in several electronic devices such as HEMTs, LEDs and high speed detectors.

C) ATOMIC LAYER EPITAXY

1) Atomic Layer Epitaxy of III-V Binary Compounds

Atomic Layer Epitaxy (ALE) of III-V semiconductors has been reported for the first time using metalorganic and hydride sources. This is achieved by using a new growth chamber and susceptor design which incorporates a shuttering mechanism to allow

successive exposure to streams of gases from the two sources. Also, most of the gaseous boundary layer is sheared off after exposure to the gas streams. GaAs and AlAs deposited by ALE are single crystal and show good optical properties.

2) Self-Limiting Mechanism in the Atomic Layer Epitaxy of GaAs

A self-limiting mechanism has been observed in the ALE of GaAs deposited by alternate exposure to AsH_3 and TMG. The thickness of the deposited film was found to be independent of the mole fraction of TMG in the gas phase. This has only been observed in the near absence of the thermal boundary layer and thus for a short exposure time to the TMG flux. A possible explanation is that the condensation coefficient of TMG can have a large value on the GaAs surface and a very small value when the surface is covered by Ga atoms.

3) Growth and Characterization of Compound Semiconductors by Atomic Layer Epitaxy

The growth of GaAs, InAs and $In_xGa_{1-x}As$ ($0 < x < .43$) by atomic layer epitaxy (ALE) has been achieved. The growth rate by ALE is found to be independent of the column III flux. ALE GaAs, grown between 450 and 630°C has been characterized by photoluminescence and Hall measurements. Initial results indicate that ALE gives improved incorporation and uniformity in the growth of InGaAs compared to conventional MOCVD and can be a suitable technique for growing ternary and quaternary layers over large areas.

D) MOLECULAR STREAM EPITAXY OF III-V COMPOUNDS

Molecular Stream Epitaxy is a new technique for the synthesis of III-V compounds. In this technique, two separate molecular streams are used, one containing column III elements and the other containing column V elements. A shutter is used to allow sequential exposure to the gas streams. We have applied this method to the growth of GaAs by MOCVD. This approach can allow (1) separation of the hydrides and metalorganics to prevent gas-phase reactions, (2) better control of layer thickness and, (3) more abrupt interfaces between layers. We have used this technique to grow GaAsP-InGaAs SLS with layers 8 Å thick and interface abruptness at least as good as those obtained from gas source MBE.

E) NEW LATERALLY SELECTIVE GROWTH TECHNIQUE BY METALORGANIC CHEMICAL VAPOR DEPOSITION

Laterally selective growth of III-V compounds has been successfully demonstrated by metalorganic chemical vapor deposition. This was achieved by suing a specially designed growth chamber and susceptor that allows the substrate to move with respect to a stationary GaAs or Si mask. We have used this technique to selectively deposit $GaAs_{1-x}P_x$ with different values of x and a GaAs - GaAsP superlattice on a single GaAs substrate. We have also selectively grown multiple color light-emitting diodes on a GaAs substrate.

Publications

1. M. A. Tischler, T. Katsuyama, N. A. El-Masry and S. M. Bedair, "Defect Reduction in GaAs Epitaxial Layers Using a GaAsP-InGaAs Strained-Layer Superlattice", Appl. Phys. Lett., 46 (3), 1 February 1985.

2. P. K. Chiang and S. M. Bedair, "p-n Junction Formation in InSb and $InAs_{1-x}Sb_x$ by Metalorganic Chemical Vapor Deposition", Appl. Phys. Lett., 46 (4), 15 February 1985.

3. S. M. Bedair, M. A. Tischler, T. Katsuyama and N. A. El-Masry, "Atomic Layer Epitaxy of III-V Binary Compounds", Appl. Phys. Lett., 47 (1), 1 July 1985.

4. G. S. Lee, Y. Lo, Y. F. Lin, S. M. Bedair and W. D. Laidig, "Growth of $InAs_{1-x}Sb_x$ ($0 < x < 1$) and InSb-InAsSb Superlattices by Molecular Beam Epitaxy", Appl. Phys. Lett., 47 (11), 1 December 1985.

5. S. M. Bedair, M. A. Tischler and T. Katsuyama, "New Laterally Selective Growth Technique by Metalorganic Chemical Vapor Deposition", Appl. Phys. Lett., 48 (1), 6 January 1986.

6. S. M. Bedair, T. P. Humphreys, P. K. Chiang and T. Katsuyama, "InAsSbBi and InSbBi: Potential Material Systems for Infrared Detection".

7. P. K. Chiang and S. M. Bedair, "Growth of InSb and $InAs_{1-x}Sb_x$ by OM-CVD", Journal of the Electrochemical Society, Vol. 131, No. 10, October 1984.

8. S. M. Bedair, T. Katsuyama, P. K. Chiang, N. A. El-Masry, M. Tischler and M. Timmons, "GaAsP-GaInAsSb Superlattices: A New Structure for Electronic Devices", Journal of Crystal Growth, 68(1984) 477-482.

9. S. M. Bedair, T. Katsuyama, M. Timmons and M. A. Tischler, "A New GaAsP-InGaAs Strained-Layer Superlattice Light-Emitting Diode", IEEE Electron Device Letters, Vol. EDL-5, No. 2, February 1984.

Conference Presentations

1) S.M. Bedair, et. al., "Growth of InSb and InAsSb by OM-CVD," Elect. Mat. Conf., Burlington, VT, June 1983.

2) W.D. Laidig, J.W. Lee, P.K. Chiang and S.M. Bedair, "Impurity-Induced Randomization of $In_sGa_{1-x}As-GaAs$ Superlattices," Electronic Materials Conference, Burlington, Vermont, June 1983.

3) S.M. Bedair, T. Katsuyama, M. Timmons, M. Tischler and N. El-Masry, "GaAsP-InGaAsSb: A New Material System for Electronic Devices," Second International Conference on OM-CVD, Sheffield, England, April 1984.

4) S.M. Bedair, T. Katsuyama, N. El-Masry and M. Tischler, "Potential Applications of GaAsP-InGaAs Superlattices," Elect. Mat. Conf., Santa Barbara, CA, June 1984.

5) M. Tischler, N. Anderson and S.M. Bedair, "Molecular Stream Epitaxy," EMC (1985), Boulder, CO.

6) G. Lee, Y. Lo, W.D. Laidig and S.M. Bedair, "Growth of $InAs_{1-x}Sb_x$ $(0 < x < 1)$ by Molecular Beam Epitaxy," EMC (1985), Boulder, CO.

7) M.A. Tischler, T. Katsuyama, D. Moore and S.M. Bedair, "A Laterally Selective Growth Technique for the Integration of Opto-electronic Devices," Third International Conference on Metalorganic Vapor Phase Epitaxy, Los Angeles, CA, April 1986, (accepted).

8) S.M. Bedair, J.K. Whisnant, N.H. Karam and N.A. El-Masry, "Laser Selective Deposition of III-V Compounds on GaAs and Si Substrate," Third International Conference on Metalorganic Vapor Phase Epitaxy, Los Angeles, CA, April 1986 (accepted).

9) M.A. Tischler, T. Katsuyama, N. Hamaguchi and N.A. El-Masry and S.M. Bedair, "Growth and Characterization of Compound Semiconductors by Atomic Layer Epitaxy," Third International Conference on Metalorganic Vapor Phase Epitaxy, Los Angeles, CA, April 1986 (accepted).

10) T. Katsuyama and S.M. Bedair, "Molecular Stream Epitaxy of III-V Compound," Electronic Material Conference, Amherst, Mass., 1986.

11) S.M. Bedair, "Defect Reduction in MBE Epilayers Using Different Superlattices." Elec. Material Conf., Amherst, Mass., 1986.

12) S.M. Bedair, et. al., "Atomic Layer Epitaxy: A New Approach for the Synthesis of III-V Compound," GaAs and Related Compounds, Las Vegas, Nevada, 1986.

13) S.M. Bedair, et. al., "In-As-Sb-Bi: A Potential Material System for Infrared Detection," MRS, 1986.

II. Personnel Partially Supported

A) Student	Degree Awarded
1) P. K. Chiang	Ph.D. 1985
2) M. Tischler	Ph.D. 1986
3) T. Katsuyama	Ph.D. 1987 (to be awarded)
4) J. Greene	MS 1986
5) D. Moore	

B) Professional Postdoctoral

1) Dr. T. Humphrey

2) Dr. N. Karam

Defect reduction in GaAs epitaxial layers using a GaAsP-InGaAs strained-layer superlattice

M. A. Tischler, T. Katsuyama, N. A. El-Masry, and S. M. Bedair
Electrical and Computer Engineering Department, Box 7911, North Carolina State University, Raleigh, North Carolina 27695-7911

(Received 30 August 1984; accepted for publication 9 November 1984)

GaAsP-InGaAs strained-layer superlattices grown lattice matched to GaAs have been used to reduce the density of threading dislocations originating from the GaAs substrate. GaAs epitaxial layers grown on the GaAsP-InGaAs superlattice buffer layers showed a dislocation density lower by at least an order of magnitude than that obtained from epitaxial layers grown directly on GaAs substrates. Transmission electron microscopy showed that dislocations originating from the GaAs substrate do not penetrate the GaAsP-InGaAs superlattice layers.

The recent advances in GaAs device and integrated circuit technology have stimulated the need for high quality, uniform substrates. These are necessary to achieve uniform circuit parameters and respectable yields. However, compound semiconductor substrates typically have several types of defects, such as dislocations, which can degrade the operation of devices and circuits. Typical substrates have dislocation densities on the order of 10^4 cm^{-2} and greater. Additionally the dislocation density is not uniform across the wafer; for example, dislocations in liquid encapsulated Czochralski (LEC) wafers usually have a W-shaped distribution, with larger densities at the edge and center of the wafer.[1] These dislocations, as evidenced by etch pits, x-ray topography, and transmission electron microscopy (TEM) have been correlated to material parameters such as photoluminescence intensity,[2,3] sheet carrier concentration, and sheet resistance[4,5] as well as device parameters including leakage[6] and drain-source[1] currents, and threshold voltage.[7-10] Sheet carrier concentration directly tracks the dislocation density while the sheet resistance is inversely proportional to it.[4] Metal-semiconductor field-effect transistor arrays across 2-in. LEC wafers show threshold voltage variations of about 400 mV [for V_{th} (mean) $= +0.126$ V] with V_{th} becoming more negative as the dislocation density increases.[7] LEC wafers typically have dislocation networks which result in large variations in device parameters while horizontal Bridgman (HB) wafers usually have more uniform dislocation densities.[11] Defect density variations across the boule can be another source of problems for GaAs technology. Thus, it is evident that the quality of the GaAs must be improved to have a viable integrated circuit process.

One possible method for reducing defects is to improve the bulk growth of GaAs. There have recently been reports[12] of HB, silicon-doped GaAs substrates with less than 200 dislocations cm^{-2}. This low density has not yet been realized in LEC or Cr-doped material, which is required for GaAs integrated circuits. The approach we have investigated is to provide a low defect density epitaxial layer using a strained-layer superlattice. This was first proposesd by Matthews and Blakeslee[13,14] who used the strain field in a GaAsP-GaAs superlattice to turn aside dislocations propagating up from the substrate. A superlattice is constructed of layers with different lattice constants such that layers are alternately under compression and tension. The layers are thinner than a maximum thickness such that the strain is accommodated elastically, but greater than a minimum thickness required for "bending over" the dislocations.[13-15] The dislocations propagating up from the substrate encounter the strain field and are bent over and forced to move laterally towards the edge of the substrate. Note that the materials must have enough lattice mismatch to generate the required strain. The problem that arises with strained-superlattice structures such as GaAs-InGaAs and GaAs-GaAsP is that they are not, as a whole, lattice matched to the GaAs substrate or epitaxial layer. Thus more dislocations are produced at these interfaces. What is needed is a superlattice composed of two materials having equal but opposite lattice mismatches, such that the average lattice constant matches that of GaAs. We have proposed a materials system, $GaAs_{1-x}P_x$-$In_yGa_{1-y}As$, which is lattice matched to GaAs when $x = 2y$.[16] Additional potential material systems are GaAsP-GaAsSb, GaAsP-InGaAsSb,[17] and $Ga_{0.52+x}In_{0.48-x}P$-$Ga_{0.52-x}In_{0.48+x}P$. This allows a high quality GaAs layer to be grown lattice matched on top of the superlattice buffer (SLB) layer. There is also some evidence that a strained superlattice may act as a gettering site for impurities out diffusing from the substrate.[18,19]

Ten period SLB's were grown by metalorganic chemical vapor deposition at atmospheric pressure in a vertical reactor. Gallium was supplied from a trimethylgallium bubbler (0 °C) at a flow rate of 5 sccm. Indium was supplied from a triethylindium bubbler (20 °C) at a flow rate of 200 sccm. AsH_3 and PH_3 (both 5% in H_2), at flow rates of 40 and 60 sccm respectively, were used as the As and P sources. Palladium diffused H_2 flowing at a rate of 4 l/m served as the carrier gas. The growth temperature was 630 °C. Four different substrates were used; two silicon doped, one Cr-doped, and one LEC (semi-insulating). All substrates were (100), oriented 2° towards (110). Details of the calibration procedure to produce the SLB lattice matched to GaAs have been previously reported.[16] For these experiments x(% P) ~ 17% and y(% In) ~ 8%. X-ray diffraction showed that the mismatch between the SLB and the GaAs substrate is less than 0.1%. The thickness of each layer is between 100–180 Å; the minimum and maximum thicknesses mentioned above are calculated (for $GaAs_{0.83}P_{0.17}$-$In_{0.08}Ga_{0.92}As$) to be on the order of 100 and 300 Å, respectively. GaAs epitaxial layers were then simultaneously grown on the SLB and directly on

 0003-6951/85/030294-03$01.00

TABLE I. Results of etch pit density measurements.

Run	Substrate	Etch pit density (cm^{-2})		
		Substrate	GaAs epilayer	SLB plus GaAs epilayer
A	Cr	$1–2 \times 10^4$	$1–8 \times 10^5$	50
B	Si	$\sim 10^4$	$\sim 10^5$	20
C	Si	$\sim 6 \times 10^4$	$\sim 10^5$	400
D	SI LEC	$1–3 \times 10^4$	$\sim 4 \times 10^5$	~ 0
E	Si	$\sim 6 \times 10^3$	$\sim 2 \times 10^5$	180

GaAs substrates for etch pit density (EPD) comparison. All the GaAs epitaxial layers were about 2 μm thick and they had mirrorlike surfaces with no cross hatching. This indicates the good lattice match between the SLB and GaAs.

Molten KOH at 330 °C was used to delineate the dislocations. Table I shows the etch pit density of the substrates, the GaAs epitaxial layers directly on the substrates, and the GaAs epitaxial layers on the 10 period SLB layers. The etch pit densities of the epitaxial samples were taken over an area about 0.5 cm square. In addition to the five sets of samples in Table I, EPD measurements were also made on five other samples. These had 10–35 superlattice periods and GaAs epitaxial layers 2–4 μm thick. The EPD's on these samples varied from 200 to 500 cm^{-2}. While EPD measurements are statistical in nature, and somewhat variable across a sample, we have consistently seen EPD's in epitaxial layers directly on GaAs substrates in the thousands per square cm range, while the SLB reduces the EPD to the hundreds per square cm range. It should be noted that this type of approach can only reduce dislocations threading up from the substrate. Dislocations produced by vacancies, interstitials, etc. within the epitaxial layer may still be present.

Transmission electron microscopy (TEM) was also done on several of the epitaxial layers on a SLB. The TEM samples were prepared by lapping and ion milling two pieces bonded together face to face. They are viewed in cross section, with the electron beam parallel to the ⟨110⟩ zone axis. Figure 1(a) shows a TEM cross section for a 10-period GaAsP-InGaAs SLB indicating the uniform thickness of the two ternary alloys. The period of the superlattice in Fig. 1(a) is about 230 Å. Figure 1(b) shows a threading dislocation which started in the GaAs substrate and does not penetrate the SLB. The SLB is delineated by the arrows. The diffraction conditions for these micrographs are not optimized for the simultaneous observation of the SLB layers and the dislocation lines. Additionally, the low dislocation density makes it quite difficult to find a dislocation using TEM. These micrographs are the results from several trials. Figure 1(c) shows another TEM cross section in which a threading dislocation does not penetrate the SLB. These TEM micrographs are another demonstration that threading dislocations which start in the substrate may not penetrate the SLB. It is not clear at this stage how many periods are required to eliminate these threading dislocations.

In conclusion, strained superlattice buffer layers have been grown with an average lattice constant equal to that of GaAs, as shown by the x-ray diffraction data. Epitaxial GaAs layers grown on these SLB's show significantly smaller dislocation densities than simultaneously grown layers directly on GaAs substrates. TEM studies show that threading dislocations which start in the GaAs substrate do not penetrate the SLB layer. It is expected that devices and circuits fabricated in epitaxial layers on top of SLB's will exhibit less variation in electrical parameters than those fabricated directly on a GaAs substrate.

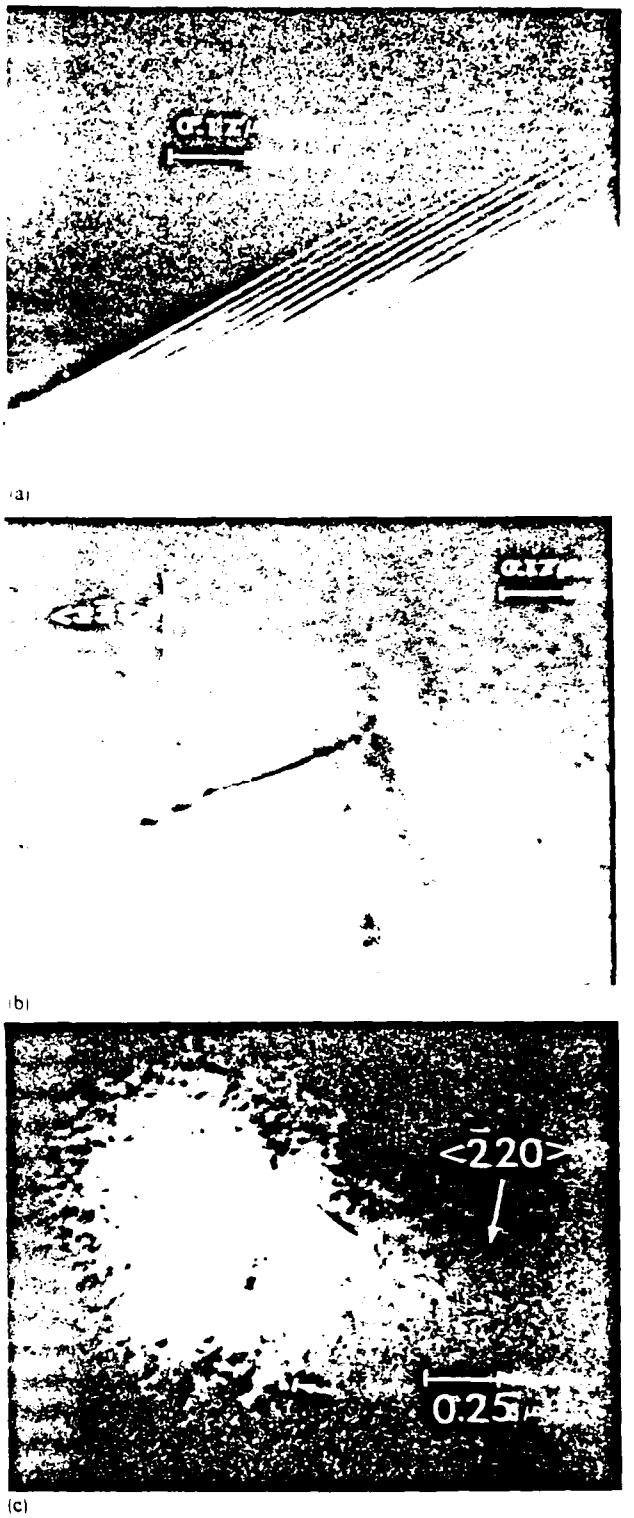

FIG. 1. (a) TEM micrograph of GaInAs-GaAsP superlattice. (b) TEM micrograph showing a threading dislocation which does not penetrate the SLB. The substrate is on the left side of the SLB. (c) TEM micrograph showing a threading dislocation which does not penetrate the SLB. The substrate is on the right side of the SLB.

This work is supported by NSF and the Army Research Office.

[1]Y. Nanishi, S. Ishida, and S. Miyazawa, Jpn. J. Appl. Phys. **22**, L 54 (1983).
[2]W. Heinke and H. J. Queisser, Phys. Rev. Lett. **33**, 1082 (1974).
[3]K. Böhm and B. Fischer, J. Appl. Phys. **50**, 5433 (1979).
[4]T. Honda, Y. Ishii, S. Miyazawa, H. Yamazaki, and Y. Nanishi, Jpn. J. Appl. Phys. **22**, L 270 (1983).
[5]H. Yamazaki, Y. Nanishi, S. Miyazawa, and Y. Ishii, GaAs Integrated Circuit Symposium, Phoenix, AZ, Oct. 25, 1983, pp. 30–33.
[6]S. Miyazawa, T. Mizutani, and H. Yamazaki, Jpn. J. Appl. Phys. **21**, L542 (1982).
[7]S. Miyazawa, Y. Ishii, IEEE Trans. Electron. Devices **ED-31**, 1057 (1984).
[8]Y. Ishii, S. Miyazawa, and S. Ishida, IEEE Trans. Electron Devices **ED-31**, 800 (1984).
[9]Y. Matsuoka, K. Ohwada, and M. Hirayama, IEEE Trans. Electron Devices **ED-31**, 1062 (1984).
[10]S. Miyazawa, Y. Ishii, S. Ishida, and Y. Nanishi, Appl. Phys. Lett. **43**, 853, (1983).
[11]Y. Ishii, S. Miyazawa, and S. Ishida, IEEE Trans. Electron Devices **ED-31**, 1051 (1984).
[12]Solid State Technol. **27**, 12 (1984), Sumitomo Company Literature
[13]J. W. Matthews, A. E. Blakeslee, and J. Mader, Thin Solid Films **33**, 253 (1976).
[14]J. W. Matthews and A. E. Blakeslee, J. Cryst. Growth **27**, 118 (1974), **29**, 273 (1975); **32**, 265 (1976).
[15]J. W. Matthews and A. E. Blakeslee, J. Vac. Sci. Technol. **14**, 989 (1977).
[16]S. M. Bedair, T. Katsuyama, M. Timmons, and M. A. Tischler, IEEE Electron Device Lett. **EDL-5**, 45 (1984).
[17]S. M. Bedair, T. Katsuyama, P. K. Chiang, N. A. El-Masry, M. A. Tischler, and M. Timmons, J. Cryst. Growth **68**, 477 (1984).
[18]W.-J. Schaff, A. S. Brown, L. F. Eastman, B. Van Rees, B. Liles, and C. Hitzman, Electronic Materials Conference, Sec. F-3, Santa Barbara, CA, June 20–22, 1984.
[19]W. T. Read, *Dislocations in Crystals* (McGraw–Hill, NY, 1953) p. 7

 0003-6951/85/030296-03$01.00

p-n junction formation in InSb and $InAs_{1-x}Sb_x$ by metalorganic chemical vapor deposition

P. K. Chiang and S. M. Bedair
Department of Electrical and Computer Engineering, North Carolina State University, Raleigh, North Carolina 27695-7911

(Received 10 August 1984; accepted for publication 19 November 1984)

p-n junctions have been fabricated in InSb and $InAs_{1-x}Sb_x$ ($0.4 < x < 0.7$) using metalorganic chemical vapor deposition. These junctions showed soft breakdown in addition to forward characteristics with a diode factor greater than 2. The ternary alloy has a cut-off wavelength in the 8–11-μm range, thus providing a potential material system for detectors covering the 8–12-μm range.

InSb and $InAs_{1-x}Sb_x$ ($0.5 < x < 0.7$) are attractive semiconductor materials for detectors covering the 3–5 and 8–12-μm spectral ranges, respectively. These two spectral ranges cover the atmospheric window where minimum absorption is present. The growth of InSb epilayers by liquid phase epitaxy (LPE)[1] and molecular beam epitaxy (MBE)[2] have been previously reported. However, previous efforts by LPE,[3] MBE,[4] and metalorganic chemical vapor deposition (MOCVD)[5,6] to grow epitaxial layers of $InAs_{1-x}Sb_x$ ($0.5 < x < 0.7$) have not been successful. Epilayers only near the binary corners have been reported. Detectors made in these composition ranges do not cover the 8–12-μm atmospheric window; thus, HgCdTe was left as the only material system that could cover this spectral range. We report here the first epitaxial growth on $InAs_{1-x}Sb_x$ ($0.4 < x < 0.7$) using MOCVD, with particular interest in the composition $x \approx 0.6$. Detectors fabricated from the $InAs_{0.40}Sb_{0.60}$ ternary alloy have a cut-off wavelength $>9\,\mu$m at a temperature >77 K. We also report *p-n* junction formation in InSb and $InAs_{1-x}Sb_x$ ($0.4 < x < 0.6$) using the MOCVD technique.

$InAs_{1-x}Sb_x$ epilayers were grown using triethylindium (TEI), trimethylantimony (TMS), and AsH_3 on GaAs, InSb, and InAs substrates, and the detailed growth conditions have been reported.[7] The as-grown material carrier concentrations are in the range of 10^{15} and 10^{16} cm^{-3} for InSb and $InAs_{1-x}Sb_x$, respectively at 77 K as deduced from Hall data for layers grown on Cr-doped GaAs. X-ray diffraction was used to obtain the InSb solid composition in $InAs_{1-x}Sb_x$. Optical transmission measurements for $InAs_{1-x}Sb_x$ epilayers on InAs or InSb substrates were per-

 0003-6951/85/040383-03$01.00

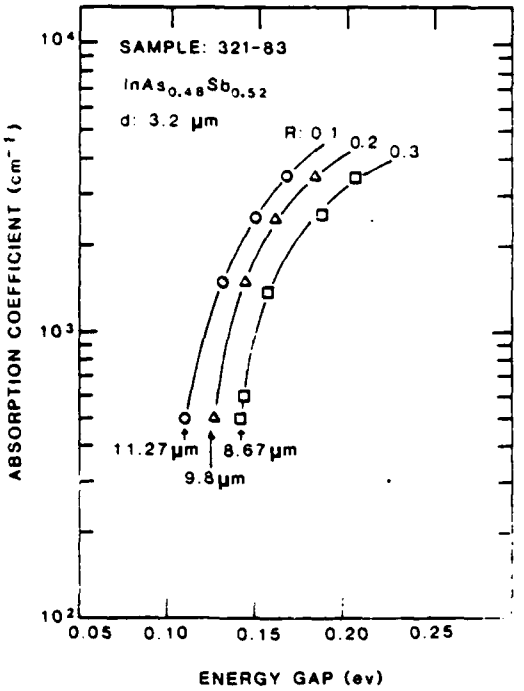

FIG. 1. Absorption coefficient vs photon energy for the $InAs_{0.48}Sb_{0.52}$ film on a (100) InAs substrate. R is the reflection coefficient.

formed by using a double-beam infrared spectrophotometer (Perkin Elmer model 983). The absorption coefficient α was obtained from the expression

$$T = \frac{(1-R)^2 \exp(-\alpha t)}{1-R^2 \exp(-2\alpha t)},$$

where t is the thickness (3.2 μm) of the epilayer, T is the transmission coefficient, and R is the reflection coefficient. The reflection coefficient R is not available for this alloy; a value of $R = 0.3$, which is appropriate for pure InAs, was used for the calculation of absorption coefficients for $InAs_{1-x}Sb_x$ in the transmission measurement. In addition, $R = 0.1$ and 0.2 were also used due to the slightly cloudy surface which may have degraded the reflectivity. The calculated absorption coefficients at room temperature for $InAs_{0.48}Sb_{0.52}$ are shown in Fig. 1 for different values of R. The cut-off wavelength or energy gap was estimated from the absorption curve by taking the wavelength or energy at which $\alpha = 500\ cm^{-1}$. This value has been used by others[7] in the optical transmission measurement. It is high enough so as not to be seriously influenced by residual absorption. Cut-off wavelength is obtained in the range 8.67–11.27 μm, depending on the value of reflection coefficient R used as shown in this figure. The cut-off wavelength for bulk grown $InAs_{0.48}Sb_{0.52}$, obtained from room-temperature optical transmission measurements, is about 11 μm.[8] This value is thus consistent with λ (cut-off) obtained from Fig. 1 with R in the range 0.1–0.2. The corresponding λ (cut-off) at 77 K for $InAs_{0.48}Sb_{0.52}$ is estimated[8] to be about 8.5 μm.

$InAs_{1-x}Sb_x$ p^+-n junctions were formed by Zn diffusion into the undoped n-type epitaxial layers. To prepare for Zn diffusion, an $InAs_{0.60}Sb_{0.40}$ sample, for example, with a 5-μm-thick n-type layer was grown on a (100)InSb substrate by MOCVD. Elemental Zn (1.70 mg) and Sb (49.79 mg) were used as the diffusion sources. The $InAs_{0.60}Sb_{0.40}$ sample and

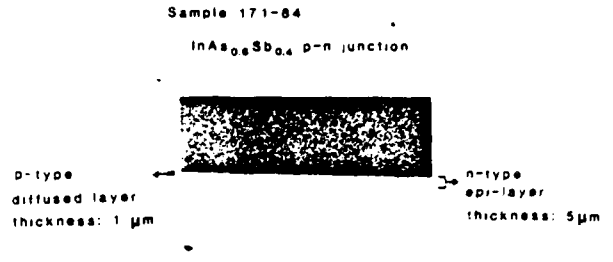

FIG. 2. Junction depth for the $InAs_{0.60}Sb_{0.40}$ p^+-n diode. 1-μm-thick p layer was formed by Zn diffusion into a 5-μm-thick n-type epilayer.

the diffusion sources were loaded into an 8-cm^3 quartz am poule, which was then evacuated to 2×10^{-6} Torr. The di fusion was carried out at 400 °C for 4 h. After diffusion, th sample was cleaved and stained in A:B solution (A—40 m H_2O + 0.3 g $AgNO_3$ + 40 ml HF, B—40 g CrO_3 + 40 m H_2O) diluted in water for a few seconds to delineate the p^+- junction. The measured junction depth was about 1 μm shown in Fig. 2.

In/Ag was used for both p^+ and n-type layers for ohmi contacts. This was done by evaporating 800 Å of In, followe by 1100 Å of Ag, and subsequent annealing at 350 °C for few minutes. Mesa diodes were fabricated using standar photolithographic techniques. Diodes were 25×25 mil^2 d lineated by an 8:1 (lactic acid: HNO_3) solution.

InSb p-n junctions were obtained either by Zn diffusio in a sealed ampoule or by direct growth of p^+ layers in t MOCVD reactor using diethylzinc (DEZn) or dimethylzin (DMZn) dopants. Since the incorporation of Zn in t MOCVD process is high for low growth temperatures, InS epilayers with a hole concentration in the 10^{19} cm^{-3} ran were obtained. Due to this limitation, p^+-n junctions we fabricated by growing a $\simeq$3-μm-thick n-type layer at 450 on a (100) InSb substrate, followed by a 0.1-μm-thick Z doped InSb, p^+ layer. The sample was then annealed 400 °C under H_2 flow for 20 min in the MOCVD reacto The metallurgical junction thickness was estimated to be the neighborhood of 0.3 μm due to Zn diffusion.

Figures 3(a), 3(b), and 3(c) show the I-V characteristi of $InAs_{0.48}Sb_{0.52}$, $InAs_{0.60}Sb_{0.40}$, and InSb p^+-n junctio with area of about 4×10^{-3} cm^2, at 77 K. Figure 4 shows t log I-V characteristics of an $InAs_{0.60}Sb_{0.40}$ p^+-n junctio with reverse impedance on the order of 10^3 Ω and with rather soft breakdown in the neighborhood of one volt. T forward characteristic shows a diode factor $n>3$ over t entire measurement range. The forward and the rever characteristics are affected by the presence of recombinati centers in the depletion region, and also due to surface lea age. It is believed that recombination centers were caused diffusion-induced damages[9] and by lattice defects resulti from lattice mismatch between the $InAs_{0.60}Sb_{0.40}$ epila and the InSb substrate.

Figure 3(c) shows the linear I-V characteristic of InSb p^+-n junction with a breakdown voltage in the neig borhood of one volt and a relatively high diode fac ($n\simeq2.7$). The forward characteristic is also determined generation and recombination mechanisms in the depleti region. These mechanisms have been indicated by Sah[10]

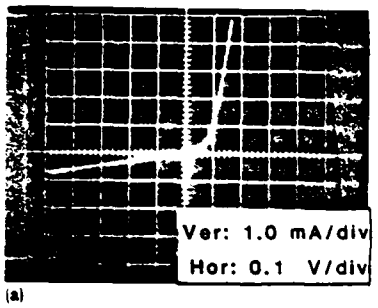

(a)

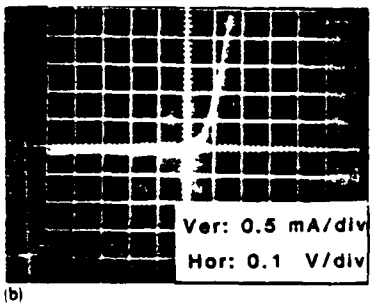

(b)

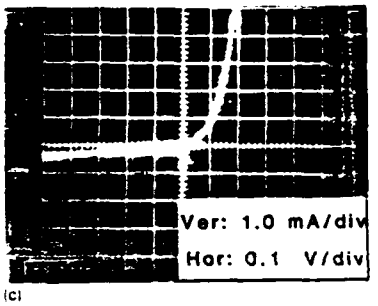

(c)

FIG. 3. I-V characteristics at 77 K of (a) $InAs_{0.48}Sb_{0.52}$, (b) $InAs_{0.60}Sb_{0.40}$, (c) InSb p^+-n diodes.

be an important effect for small band-gap materials such as InSb at low temperatures. It is also believed that the surface recombination can also result in a high diode factor, especially for the shallow junction. The reverse characteristics will be controlled by generation-recombination and band-to-band tunneling mechanisms at small and large bias, respectively.[11]

Detailed study performed on InSb p^+-n junction indicated that up to a reverse bias voltage of one volt, the I-V characteristic can be represented by the recombination-generation current. For the reverse voltage greater than one volt, the tunneling current was dominant. This study showed good agreement between the present experimental results and theoretical calculations and will be available elsewhere.[12] We believed that the same trend can also be applied to the junctions built in $InAs_{1-x}Sb_x$ due to small effective mass and band gap[11] for this ternary compound.

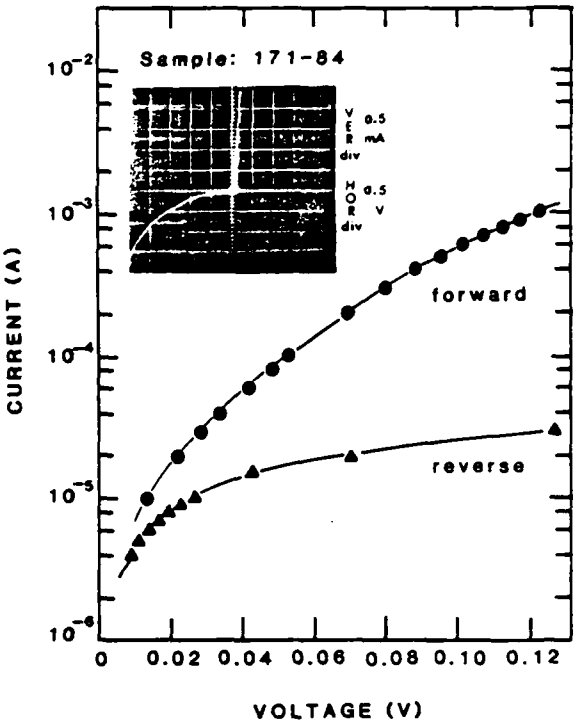

FIG. 4. Log I-V characteristics of the $InAs_{0.60}Sb_{0.40}$ p^+-n diode at 77 K.

In conclusion, MOCVD has been used to grow epitaxial layers of InSb and $InAs_{1-x}Sb_x$ $(0.4 < x < 0.7)$ on InSb substrates for the first time. p-n junctions have been fabricated in both the binary and ternary compounds. Optical transmission measurements showed that $InAs_{1-x}Sb_x$ can have a cut-off wavelength in the 8–11-μm spectral range. Detectors fabricated from these junctions can cover the 3–5-μm and part of the 8–12-μm spectral range. Thus InAsSb can be a useful alternative to the CdHgTe material system.

We would like to thank Dr. W. D. Laidig, Dr. G. Lucovsky, Dr. Steven Jost, and Mr. T. Katsuyama for their assistance in this work. This work was supported by NASA and Army Office of Research grants.

[1]D. E. Holmes and G. S. Kamath, J. Electron. Mater. **9**, 95 (1980).
[2]A. J. Noreika, W. J. Takei, M. H. Froncombe, and C. E. C. Woods, J. Appl. Phys. **53**, 4932 (1982).
[3]G. B. Stringfellow and P. E. Greene, J. Electrochem. Soc. **118**, 805 (1971).
[4]W. J. Schaffer, 3rd MBE Workshop University of California, Santa Barbara, 1981.
[5]T. Fukui and Y. Horikoshi, Jpn. J. Appl. Phys. **19**, L53 (1980).
[6]G. Nataf and C. Verie, J. Cryst. Growth **55**, 87 (1981).
[7]P. K. Chiang and S. M. Bedair, J. Electrochem. Soc. **131**, 2422 (1984).
[8]J. C. Woolley and J. Warmer, Can. J. Phys. **42**, 1879 (1964).
[9]R. L. Mozzi and J. M. Lavine, J. Appl. Phys. **41**, 280 (1970).
[10]C. T. Sah, IRE Trans. Electron Devices **ED-9**, 94 (1962).
[11]R. D. Thom, T. L. Koch, J. D. Lagan, and W. J. Parrish, IEEE Trans. Electron Devices **ED-27**, 160 (1980).
[12]P. K. Chiang, Ph.D. thesis, North Carolina State University, 1985.

Atomic layer epitaxy of III-V binary compounds

S. M. Bedair, M. A. Tischler, T. Katsuyama, and N. A. El-Masry
Electrical and Computer Engineering Department, Box 7911, North Carolina State University, Raleigh, North Carolina 27695-7911

(Received 20 March 1985; accepted for publication 17 April 1985)

Atomic layer epitaxy (ALE) of III-V semiconductors is reported for the first time using metalorganic and hydride sources. This is achieved by using a new growth chamber and susceptor design which incorporates a shuttering mechanism to allow successive exposure to streams of gases from the two sources. Also, most of the gaseous boundary layer is sheared off after exposure to the gas streams. GaAs and AlAs deposited by ALE are single crystal and show good optical properties.

The recent interest in high electron mobility transistors (HEMT's), superlattices, and quantum well structures and devices has required improvements in the ability to produce thin layers and abrupt interfaces. Both molecular beam epitaxy (MBE) and, to a lesser extent, metalorganic chemical vapor deposition (MOCVD) have made impressive advances in this respect and yet both are limited by operating in a "bulk" growth regime. The ultimate control of the growth of III-V compounds would be achieved by the deposition of one monolayer of column III atoms followed by a monolayer of column V atoms. This process would then be repeated until the desired thickness has been reached. The total layer thickness could be controlled very accurately since each cycle of exposures would result in the growth of a known thickness. The interfaces, in principle, would be atomically abrupt since the reactant fluxes could be changed within one atomic layer. The atomic layer epitaxy (ALE) of III-V compounds could be achieved using either MBE or MOCVD. In the case of MBE, the shutters are assumed to allow the exposure of the substrate to either column III or V beams independently. In the case of MOCVD, an analogous shuttering mechanism would be used.

We report for the first time the successful atomic layer epitaxy of GaAs and AlAs by MOCVD. This technique can also be used to investigate the MOCVD growth mechanism and will be reported on at a later date. The growth chamber is schematically shown in Fig. 1. For the growth of GaAs, $AsH_3 + H_2$ and trimethylgallium (TMG) + H_2 flow through the inlet tubes *A* and *B*, respectively. A large flow of H_2 in the middle tube (*C*) is designed to prevent mixing of the gases from tubes *A* and *B*. The rf heated susceptor is made of graphite coated with silicon carbide, and consists of several

 0003-6951/85/130051-03$01.00

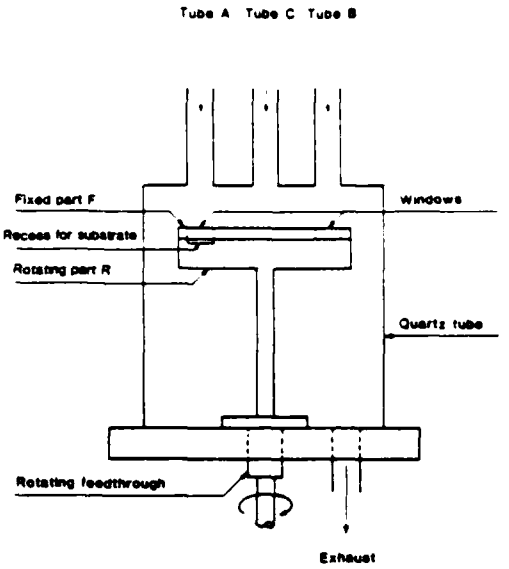

FIG. 1. Schematic diagram of the growth chamber and susceptor for ALE. The susceptor consists of a fixed part *F*, a rotating part *R*, and a recess in part *R* which holds the substrate. Inlet tubes *A* and *B* provide the reactant gases. A large H_2 flow in tube *C* helps prevent mixing of the gases from tubes *A* and *B*.

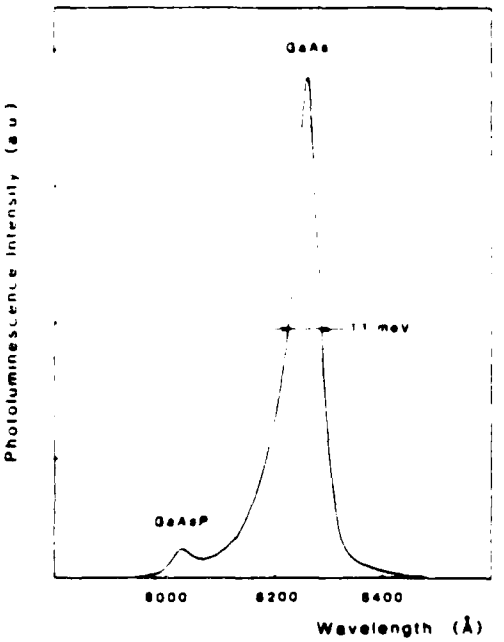

FIG. 2. Photoluminescence at 77 K of 100 cycles of GaAs grown by ALE sandwiched between layers of $GaAs_{0.97}P_{0.03}$. The full width at half-maximum is 11 meV.

parts. Fixed part *F* has two windows aligned to face the inlet tubes *A* and *B*. The substrate sits in a recess in the rotating part *R* and can be positioned under the windows of the fixed part *F*, thus facing either the column III or V input flux. The position of the substrate is controlled through a rotating feedthrough at the base of the growth chamber. The recess in part *R* and the thickness of the substrate are chosen to allow minimum clearance between the substrate surface and the fixed part of the susceptor. When the substrate is exposed to the stream of column *III* species from inlet *B*, a boundary layer will build up on the substrate surface. When the substrate is rotated away from this position, most of the boundary layer will be sheared off by the fixed part *F*, allowing an almost immediate termination of exposure of the substrate to the input flux. Additionally, the initial substrate exposure to the column III flux will take place almost without the presence of any gaseous boundary layer (made up of $H_2 + AsH_3$ in this case). The above arguments can also be applied when the substrate is moved under tube *A* and exposed to AsH_3. Thus, for a short exposure time, it is possible that the adsorption process is controlled by surface kinetics rather than diffusion of the reactant species through a boundary layer, as is always the case in conventional MOCVD growth.[1]

This technique was used to deposit GaAs and AlAs. In the case of GaAs, AsH_3 (5% in H_2) + 500 sccm of H_2 and trimethylgallium (TMG) + 500 sccm of H_2 flowed through tubes *A* and *B*, respectively. The flow of H_2 through the TMG bubbler and the temperature of the bubbler were set to 0.5 sccm and − 15 °C respectively which are the minimum values available in our system. The flow of AsH_3 was 10 sccm. Three liters per minute of H_2 flowed through the center tube (*C*) to prevent mixing. The substrate temperature was in the range of 560–600 °C. All substrates were *n*-type GaAs, (100), oriented 2° towards (110). The growth process starts by heating the substrate under AsH_3 (tube *A*) for a few minutes. The substrate is then exposed to the TMG (tube *B*) for 1 s and then moved back under the AsH_3 for 5 s. One complete cycle was performed in about 10 s. All growths consisted of 100 cycles. The exposure time to AsH_3 is not critical since excess As atoms will evaporate almost immediately. The sticking probability of As on GaAs covered with Ga is very close to unity.[2] After the first monolayer of As is adsorbed, its sticking probability reduces to almost zero. The growth of AlAs was carried out in an analogous manner using trimethylaluminum (TMA) at 9 °C and a flow of H_2 through the bubbler of 2.5 sccm.

The ALE samples of GaAs were characterized by photoluminescence (PL) at 77 K. Two types of samples were grown. One consisted of 100 cycles of GaAs grown by ALE on a 3-μm-thick InGaAs-GaAsP superlattice grown by conventional MOCVD.[3] The superlattice is lattice matched to GaAs and has an effective band gap of about 1.3 eV. The second type of sample consisted of a 2-μm-thick $GaAs_{0.97}P_{0.03}$ layer, 100 cycles of GaAs by ALE, and a 300–500-Å $GaAs_{0.97}P_{0.03}$ cap. The $GaAs_{0.97}P_{0.03}$ layers were grown by conventional MOCVD. This was achieved by adding a second TMG and PH^3 sources to line *A*. The superlattice and the thick $GaAs_{0.97}P_{0.03}$ layer prevented photoluminescence from the GaAs substrate from interfering with the signal from the ALE GaAs layer. The cap layer facilitated cross-sectional thickness measurements.

Figure 2 shows the PL spectra of the latter type of sample with 100 cycles of ALE GaAs. The GaAs peak is clearly evident and has a full width at half-maximum of about 11 meV indicating the good quality of the GaAs grown by ALE. The small peak is from the $GaAs_{0.97}P_{0.03}$ layer. The former type of sample also showed a GaAs peak. The AlAs samples consisted of 2 μm of GaAs, 100 cycles of AlAs, and a 1000-Å GaAs cap. The GaAs in this case was also grown by conventional MOCVD.

Figure 3 shows the surface of a GaAs layer grown by ALE. All the deposited layers had mirrorlike surfaces.

FIG. 3. Photomicrograph of the surface of 100 cycles of GaAs grown by ALE.

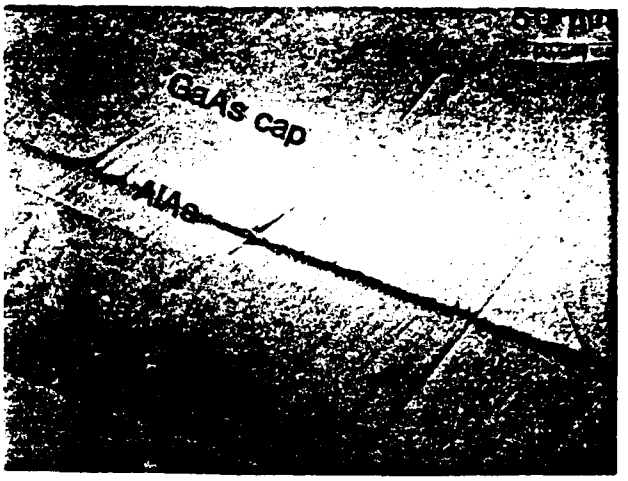

FIG. 4. Photomicrograph of 100 cycles of AlAs grown by ALE sandwiched between layers of GaAs, and angle lapped at 1/3°.

Transmission electron microscope (TEM) samples were prepared by lapping and ion milling two pieces which were bonded together face to face. They were viewed in cross section with the electron beam parallel to the ⟨002⟩ zone axis. Diffraction studies by TEM indicated that the ALE growths are single crystal. The GaAs layer is about 800 Å thick as measured by TEM. Figure 4 shows an AlAs sample angle lapped at 1/3°. The dark line is the AlAs layer grown by ALE. It is about 300 Å thick.

The difference in thicknesses between ALE GaAs and AlAs is a result of the flux of the column III species. Ideally, 100 cycles, each depositing one monolayer of column III and one monolayer of column V species, would produce a layer about 283 Å thick. However, the minimum fluxes available were system limited with the TMG flux several times larger than the TMA flux. Additionally the minimum reproducible exposure time was one second. Thus for ALE of GaAs, about two to three monolayers of Ga were deposited on the surface, whereas in the case of AlAs about one atomic layer of Al was deposited. The use of triethylgallium, with its lower vapor pressure, should allow the deposition of single layers of gallium. The deposition of more than one monolayer is not present in the ALE of II-VI compounds[4] due to the very high vapor pressure of the species.

In order to make sure that conventional MOCVD growth was not occurring from any mixing of gases in the growth chamber, the following experiment was carried out. The substrate was exposed to the TMG stream for 3 min while the AsH_3 and center H_2 lines were flowing as described above. The deposited film had a dull surface and could be wiped off by a cotton swab. PL on this layer deposited on a superlattice substrate showed only a very weak GaAs peak. The corresponding experiment with a superlattice substrate exposed only to AsH_3 with the TMG and center H_2 lines flowing showed no GaAs PL peak. Thus, the amount of mixing is quite small and is not expected to play a significant role in the ALE process.

The ALE method gives more insight into the MOCVD process. Several models for the deposition mechanism have been proposed. For example, one model proposed that the metalorganic molecule and the hydride adsorb on separate surface sites, followed by the formation of intermediate complexes and then the desorption of methane.[5] Another model showed that intermediate complex formation takes place in the gas phase.[6] It was also proposed that complete reaction in the gas phase takes place followed by the successive diffusion of small GaAs clusters towards the surface.[7] However, the result of the current experiment clearly indicates that MOCVD can also take place through independent deposition of Ga and As species.

In conclusion, ALE of GaAs and AlAs has been demonstrated by MOCVD for the first time. This has been accomplished by using a new design for the growth chamber and susceptor. The susceptor incorporates a shuttering action which allows the substrate to be sequentially exposed to different gas streams and also shears off most of the boundary layer which builds up during exposure. The current results also indicate that the growth by MOCVD takes place through the independent deposition of both Ga and As species. We believe that atomic layer epitaxy will be useful for growing structures and devices requiring very well controlled thicknesses and/or very abrupt interfaces. Additionally, ALE may provide a vehicle for investigating fundamental aspects of compound semiconductor growth.

This work was supported by Army Office of Research and Air Force Office of Scientific Research.

[1] M. R. Leys and H. Veenvliet, J. Cryst. Growth **55**, 145 (1981).
[2] J. R. Arthur, J. Appl. Phys. **39**, 4032 (1968).
[3] S. M. Bedair, T. Katsuyama, M. Timmons, and M. A. Tischler, Electron Device Lett. **5**, 45 (1984).
[4] M. Pessa, P. Huttunen, and M. A. Herman, J. Appl. Phys. **54**, 6047 (1983).
[5] D. J. Schlyer and M. A. Ring, J. Electrochem. Soc. **124**, 569 (1977).
[6] W. H. Petzke, V. Gottschalch, and E. Butter, Kristall Tech. **9**, 763 (1974).
[7] I. A. Frolov, P. B. Boldyrevskii, B. L. Druz, and E. B. Sokolov, Inorg. Mater. **13**, 632 (1977).

Growth of $InAs_{1-x}Sb_x$ ($0 < x < 1$) and InSb-InAsSb superlattices by molecular beam epitaxy

G. S. Lee, Y. Lo, Y. F. Lin, S. M. Bedair, and W. D. Laidig
Department of Electrical and Computer Engineering, North Carolina State University, Raleigh, North Carolina 27695-7911

(Received 20 June 1985; accepted for publication 26 September 1985)

Thin films of $InAs_{1-x}Sb_x$ ($0 < x < 1$) have been deposited on GaAs and InSb substrates in the temperature range 300–400 °C using molecular beam epitaxy. The solid composition was found to be quite sensitive to the Sb flux and less sensitive to As flux. InSb-InAsSb superlattice structures have also been grown and studied. Both the ternary alloy and the superlattice structures can be potential material systems for detectors covering the 8–12-μ range.

Recently there has been extensive interest for detectors covering the 8–12-μm spectral range where minimum atmospheric absorption is present. Although the HgCdTe material system plays the major role for detectors covering this spectral range, $InAs_{1-x}Sb_x$ ternary alloys with $x \simeq 0.6$ can offer an attractive alternative for detectors covering part of the 8–12-μm spectral range. $InAs_{0.4}Sb_{0.6}$ has the lowest band gap ($E_g = 0.1$ eV at room temperature) of the III-V compound semiconductors.[1] Thus detectors built from this alloy can have a cut-off wavelength λ_c of about 12 and 9 μm at room temperature and 77 K, respectively. Previous efforts to grow epitaxial layers of $InAs_{0.4}Sb_{0.6}$ by liquid phase epi-

 0003-6951/85/231219-03$01.00

taxy (LPE)[2] and molecular beam epitaxy (MBE)[3] have been only marginally successful. Recently, however, InAsSb has been epitaxially grown using metalorganic chemical vapor deposition (MOCVD).[4,5] In addition, the fabrication of *p-n* junctions in this ternary alloy has been reported.[6] However, at 77 K, further reduction in the band gap of the $InAs_{0.4}Sb_{0.6}$ is necessary for detectors based on this ternary alloy to cover the entire 8–12-μm range. This can be achieved using the following approach. When a net tensile strain is applied to $InAs_{0.4}Sb_{0.6}$ further reduction in the band gap can be achieved. Such strain can be achieved when a thin $InAs_{0.4}Sb_{0.6}$ film is sandwiched between two InSb films. Thus, an InSb-$InAs_{0.4}Sb_{0.6}$ multilayer structure or a strained layer superlattice (SLS) can result in necessary band-gap reduction to allow detectors built with the SLS structure to cover the 8–12-μm range. Calculations predicting band-gap values for the $InAs_{1-x}Sb_x$-$InAs_{0.4}Sb_{0.6}$ ($x > 0.6$) have been reported by Osbourn.[7] We describe here the epitaxial growth of $InAs_{1-x}Sb_x$ in the composition range $0 < x < 1$ using MBE. We also report our initial results on the synthesis of InSb-InAsSb SLS. MBE can be a quite suitable technique for the growth of the ternary and the SLS due to its ability for thickness control and deposition at relatively low temperature.

The epitaxial growth was carried out in a Varian 360 system using both GaAs and InSb substrates. The GaAs and InSb substrates were etched prior to growth in 7:1:1 (H_2SO_4:H_2O_2:H_2O) and 8:1 (lactic:HNO_3), respectively. The source materials were elemental In, Sb, and As. Beam equivalent pressures (BEP) were measured under growth conditions by interposing an ion gauge flux monitor to intercept the molecular beam. The measured BEP, when corrected by the background pressure, is assumed to be proportional to the In, Sb_4, and As_4 fluxes incident on the substrate surface. Predeposition heating of both InSb and GaAs substrates at 450 °C under Sb_4 overpressure was found to be adequate.

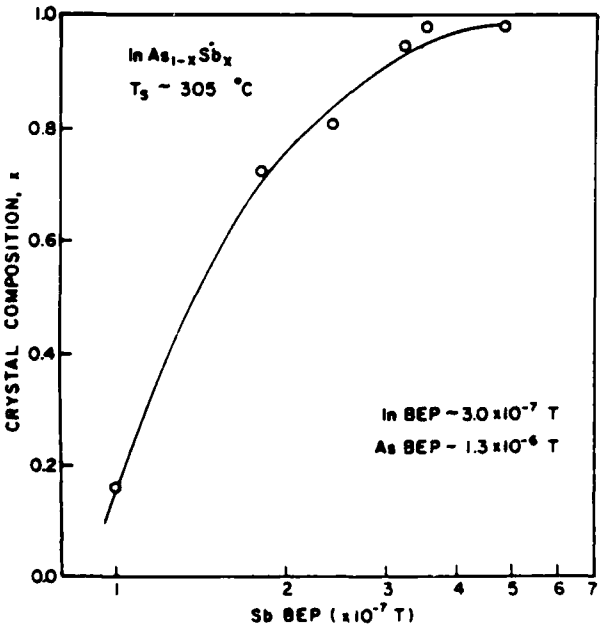

FIG. 1. Crystal composition x of $InAs_{1-x}Sb_x$ vs Sb BEP at a substrate temperature of 305 °C.

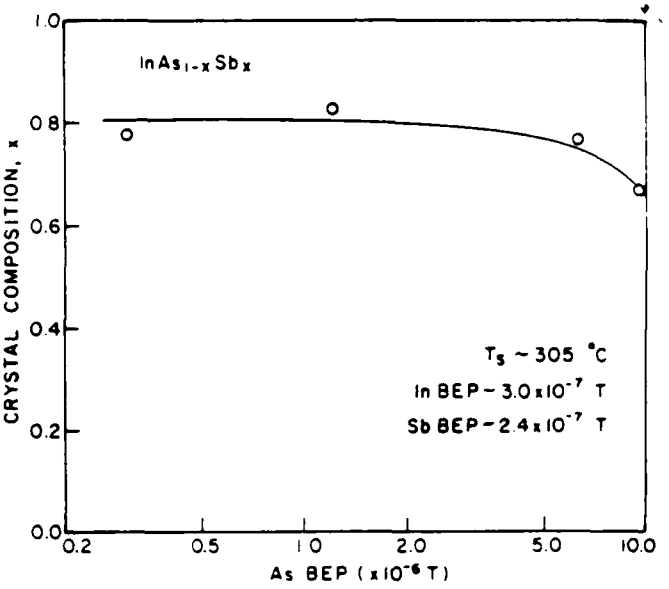

FIG. 2. Crystal composition x of $InAs_{1-x}Sb_x$ as a function of As beam equivalent pressure (BEP) at a substrate temperature of 305 °C.

Deposition was carried out with substrate temperatures in the range of 300–400 °C. The In flux was adjusted to deposit about 0.6 μm/h. X-ray diffraction was used to identify the deposition of InSb on GaAs substrate and the composition (x) of the $InAs_{1-x}Sb_x$ ternary compounds.

The first set of experiments was carried out at substrate temperature $T_s = 305$ °C to study the effect of Sb on the composition x, for given fluxes of In and As. Figure 1 shows the variation in the value of x with Sb BEP for the case when the BEP's of In and As were kept constant at 3×10^{-7} Torr and 1.3×10^{-6} Torr, respectively. As shown in this figure, changing the Sb flux can result in solid composition in the range $0 < x < 1$; however, the value of x is very sensitive to Sb flux especially for low values of x. The second set of experiments was carried out to study the effect of As flux on the value of x for constant In and Sb fluxes. Figure 2 shows that the value of x is not very sensitive to the As flux. There was almost no variation in the value of x as a result of changing

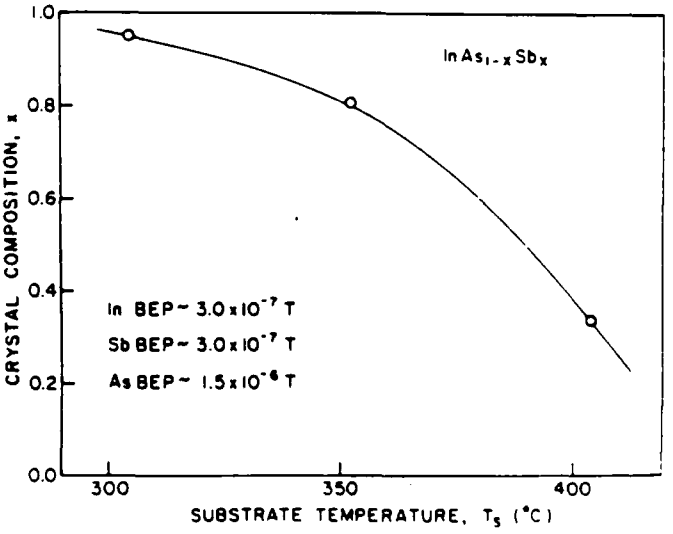

FIG. 3. Dependence of the crystal composition x of $InAs_{1-x}Sb_x$ on the substrate temperature.

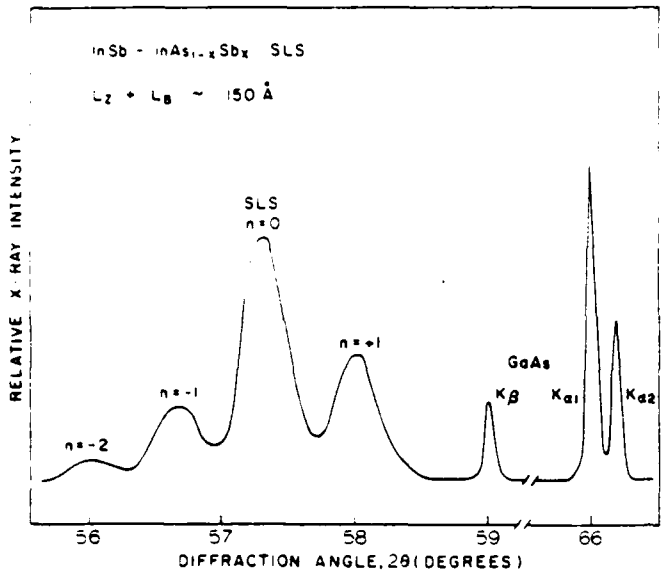

FIG. 4. X-ray diffraction pattern of strained layer superlattice with alternating layers of $x \sim 0.74$ $InAs_{1-x}Sb_x$ and InSb.

the As BEP by a factor of 50, using In and Sb BEP's of 3×10^{-7} Torr and 2.4×10^{-7} Torr, respectively. We have also observed that the surface morphology of $InAs_{1-x}Sb_x$ film, for a given value of x, deteriorates with excessively high As flux. Thus, from Figs. 1 and 2, it seems that varying in the Sb flux is more effective in controlling the solid composition of this ternary alloy. The third set of experiments was performed at different substrate temperatures and for fixed values of In, As, and Sb BEP of 3×10^{-7}, 1.5×10^{-6}, and 3×10^{-7} Torr, respectively. Higher values of x can be achieved at low substrate temperatures as shown in Fig. 3. Similar observations were reported on the MOCVD growth of $InAs_{1-x}Sb_x$.[4] Thus, adjusting the substrate temperature may offer a convenient way of controlling the solid composition, especially for low values of x.

An InSb-InAsSb SLS was deposited on a GaAs substrate at $T_s = 350$ °C. The BEP of In, Sb, and As was kept at 3×10^{-7}, 3.1×10^{-7}, and 1.3×10^{-6}, respectively. The SLS was grown by keeping the substrate exposed to In and Sb fluxes at all the times, while the As shutter was microprocessor controlled for the deposition of InAsSb and InSb, respectively. Growth times of InSb and InAsSb were adjusted to 33 and 67 s, respectively. Ninety periods were deposited, resulting in a total thickness of 1.5 μm as measured from a cleaved cross section. The period of the SLS is approximately 150 Å, consisting of 50 Å of InSb and 100 Å of InAsSb. This is consistent with growth rates from thicker calibration samples InSb and InAsSb. Figure 4 shows the x-ray diffraction pattern of the InSb-InAsSb SLS structure. The zero-order diffraction, $n = 0$, gives the average lattice parameter of the SLS, although this does not correspond directly to the average composition of SLS. The average composition was obtained from an electron microprobe (EMP) measurement on the entire SL structure. EMP shows that on the average the SL has 8.8 at. % of As. Due to the thickness ratio of the individual layers this will correspond to about 13 at. % of As in the ternary alloy, i.e., $x = 0.74$. The satellite peaks located for example at $n = \pm 1$ are due to the periodicity of the structure,[8,9] and indicate a period of about 150 Å. This is consistent with the value obtained from the total thickness of the 90 periods and is also in agreement with our predicted growth rates.

In conclusion, thin films of $InAs_{1-x}Sb_x$ have been deposited on GaAs and InSb substrates over the composition range $0 < x < 1$. The composition of the solid film was found to be fairly sensitive to both the growth temperature and the Sb flux, but much less sensitive to the As flux. In addition, it has been demonstrated that the growth of InSb-InAsSb superlattices is possible. Results for an InSb-$InAs_{0.26}Sb_{0.74}$ SLS with 150-Å-thick periods have been described. These InAsSb ternary and the InSb-InAsSb SLS structures should have potential applications for detectors covering the 8–12-μm spectral range.

This work is supported by the National Science Foundation and the Army Office of Research.

[1] J. C. Woolley and J. Warner, Can. J. Phys. **42**, 1879 (1964).
[2] G. B. Stringfellow and P. E. Greene, J. Electrochem. Soc. **118**, 805 (1971).
[3] W. J. Schaffer, Third MBE Workshop, University of California, Santa Barbara (1981).
[4] P. K. Chiang and S. M. Bedair, J. Electrochem. Soc. **131**, 2422 (1984).
[5] T. Fukui and Y. Horikoshi, Jpn. J. Appl. Phys. **19**, L53 (1980).
[6] P. K. Chiang and S. M. Bedair, Appl. Phys. Lett. **46**, 383 (1985).
[7] G. C. Osburn, J. Vac. Sci. Technol. B **2**, 176 (1984).
[8] W. D. Laidig, C. K. Peng, and Y. F. Lin, J. Vac. Sci. Technol. B **2**, 181 (1984).
[9] M. Quillec, L. Goldstein, G. LeRoux, J. Burgeat, and J. Primot, J. Appl. Phys. **55**, 2904 (1984).

New laterally selective growth technique by metalorganic chemical vapor deposition

S. M. Bedair, M. A. Tischler, and T. Katsuyama
Electrical and Computer Engineering, North Carolina State University, Raleigh, North Carolina 27695-7911

(Received 17 June 1985; accepted for publication 10 October 1985)

Laterally selective growth of III-V compounds has been successfully demonstrated by metalorganic chemical vapor deposition. This was achieved by using a specially designed growth chamber and susceptor that allows the substrate to move with respect to a stationary GaAs or Si mask. We have used this technique to selectively deposit $GaAs_{1-x}P_x$ with different values of x and a GaAs-GaAsP superlattice on a single GaAs substrate. We have also selectively grown multiple color light-emitting diodes on a GaAs substrate.

Integrated optical and electronic devices require the fabrication of many different components, each with its own material and structural requirements, on one chip. Optimum performance of integrated devices necessitates separate structures which fulfill the material, thickness, and doping requirements of each type of device. Current activities in this integrating process have mainly relied on the same multilayer structure to fabricate the different optical and microwave components.[1-3] Thus a single or multilayer structure that can be optimum for one particular device, a field-effect transistor (FET) for example, will not satisfy the device structure required for a detector or laser. This restriction imposes severe limitations on the integration of different components, such as lasers, light-emitting diodes (LED's), modulators, detectors, and FET's. Previous efforts to reduce such limitations have been based on compromises between different device structures or by selective etching[1] to remove unwanted layers or ion implantation[4] to selectively dope different device structures. The necessary processing usually requires several separate growth steps as well as masking, etching, and lift-off, which may result in a low yield. Selective area growth by molecular beam epitaxy (MBE) using a movable shadow mask to achieve epitaxial writing of GaAs has also been reported.[5] However, multilayer writing using this technique can be difficult due to the requirements of precise registration inside the MBE chamber.[5] Selective growth by both MBE[6] and metalorganic chemical vapor deposition (MOCVD)[7] through windows in SiO_2 has also been reported; however, the same layered structure is deposited in each area. The ideal situation is to deposit different structures on selected areas of the substrate. These structures can be tailored to achieve optimum performance for the different devices.

We report here, for the first time, initial and promising results to achieve such goals. Laterally selective growths of different material systems and multilayer structures are deposited on a GaAs substrate using MOCVD. This is achieved by a new susceptor design that allows relative motion between a GaAs substrate and a GaAs mask.

The experimental setup is shown in Fig. 1. The rf heated susceptor is made of graphite coated with silicon carbide and consists of several parts. Fixed part F has a window in which the GaAs mask is located. The GaAs substrate sits in a recess in the rotating part R. The position of the substrate, with respect to the opening in the GaAs mask, is controlled by rotating part R using a feedthrough at the base of the growth chamber. The reactant gases are introduced into the growth chamber through an inlet tube which directly faces the window and mask located in the fixed part F. This will allow the substrate to be exposed to a direct stream of the reactant gases. The recess in part R and the substrate thickness are chosen to allow minimum clearance between the substrate and GaAs mask.

Selective epitaxy is achieved by exposing part of the substrate to the incoming gas stream; the rest of the substrate is covered either by the GaAs mask or by a portion of the fixed part, F. The desired structure, made of single or multiple layers, with the desired material, thickness, and doping specifications, can thus be epitaxially grown on this unmasked area. The substrate can then be rotated to mask the already grown structure and expose a new part of the substrate on which a different structure may be deposited. Such a process can be continued, as necessary, to selectively grow any number of structures that are needed. We have demonstrated this new growth process by selectively depositing GaAs, $GaAs_{1-x}P_x$, $GaAs_{1-y}P_y$, and GaAs-Ga(AsP) su-

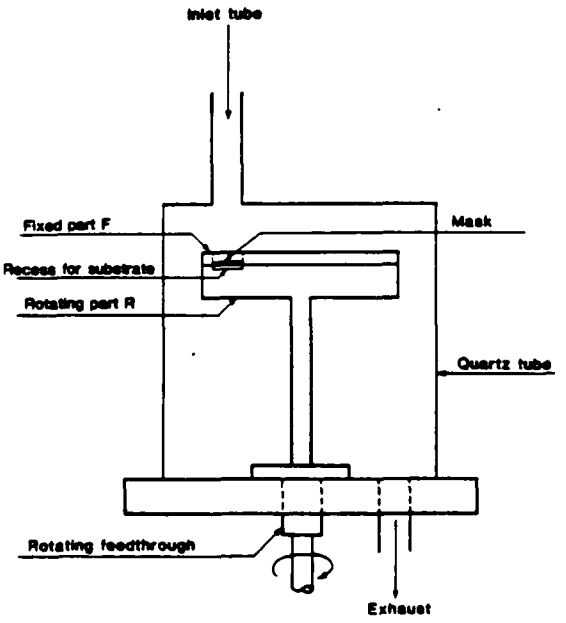

FIG. 1. Experimental setup for selective epitaxy. The substrate is located in the recess in rotating part R. Fixed part F has a window in it in which the GaAs mask is placed. The reacting gases enter through the inlet tube and flow directly onto the mask and substrate.

 0003-6951/86/010030-03$01.00

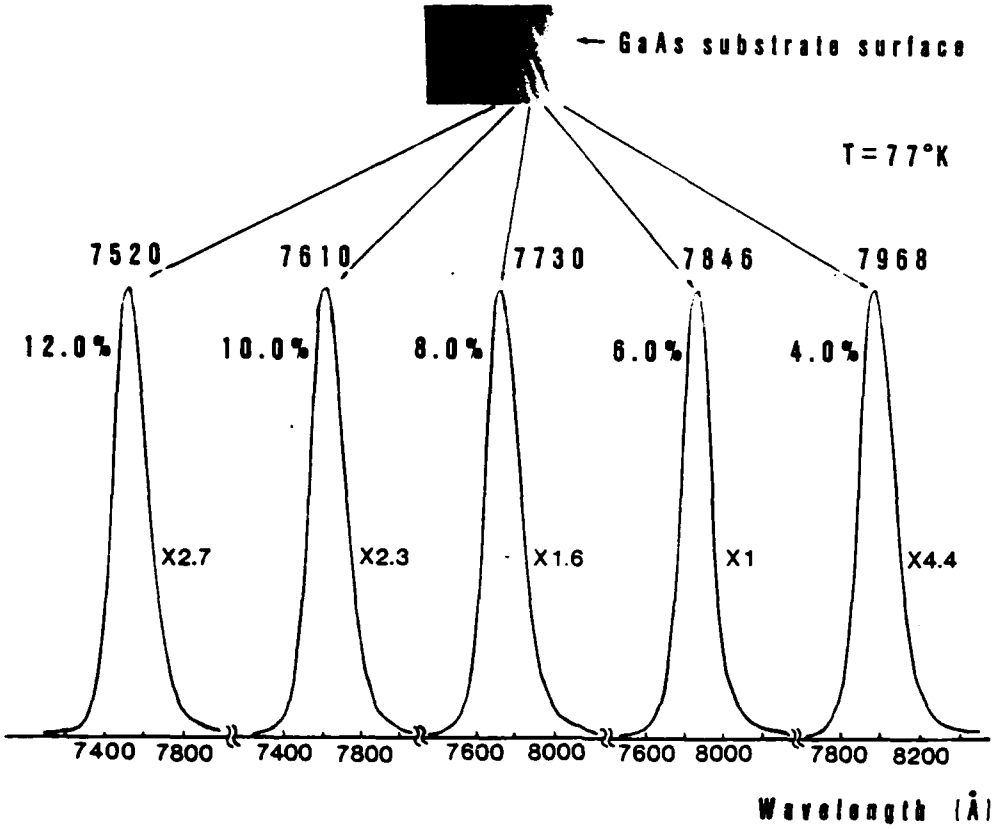

FIG. 2. Surface morphology and photoluminescence spectra for five layers of selectively grown $GaAs_{1-x}P_x$ with $x = 4, 6, 8, 10$, and 12%. The numbers beside each spectra are the intensity normalization factors.

perlattice structures on a single GaAs substrate.

The GaAs substrates were (100), oriented 2° towards (110), and the growth temperature was 650 °C. AsH_3, PH_3, and trimethylgallium (TMG) were used as sources for As, P, and Ga, respectively. The *n*- and *p*-type dopants were H_2Se and dimethylzinc (DMZ), respectively. The first set of experiments utilized a mask with an opening about 1 cm long and 1000 μm wide. Five $GaAs_{1-x}P_x$ layers were selectively grown with different values of x. Different atomic percent of GaP in these layers was achieved by changing the PH_3 mole fraction in the gas phase, while those of AsH_3 and TMG were kept constant. Photoluminescence (PL) at 77 K was used to determine the value of x for the different layers. Figure 2 shows the surface of the selectively grown $GaAs_{1-x}P_x$ layers for $x = 4, 6, 8, 10$, and 12%. The PL spectra of each of these selectively grown areas are also shown in Fig. 2. Figure 3 shows a photomicrograph of these layers, showing that their width in this region is about 600 μm each.

The compositional variation across the selected growth regions has been studied using scanning PL. The sample was mounted in a cryostat and cooled to 77 K. An Ar^+ ion laser beam is scanned across the sample in 25-μm steps. The variation, for a typical sample, of PL peak wavelength with position is plotted in Fig. 4. The flat regions in Fig. 4 correspond to areas with uniform composition and their PL spectra are quite sharp. In the transition regions (between two areas of different, but uniform composition) the PL spectra are

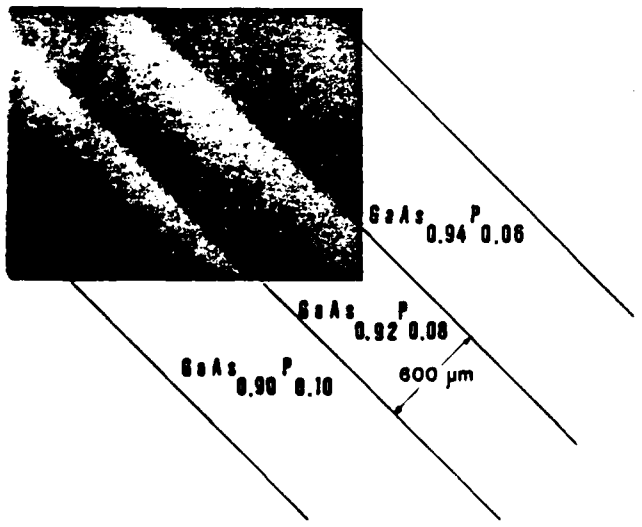

FIG. 3. Photomicrograph of three layers of selectively grown $GaAs_{1-x}P_x$ with $x = 6$, 8, and 10%.

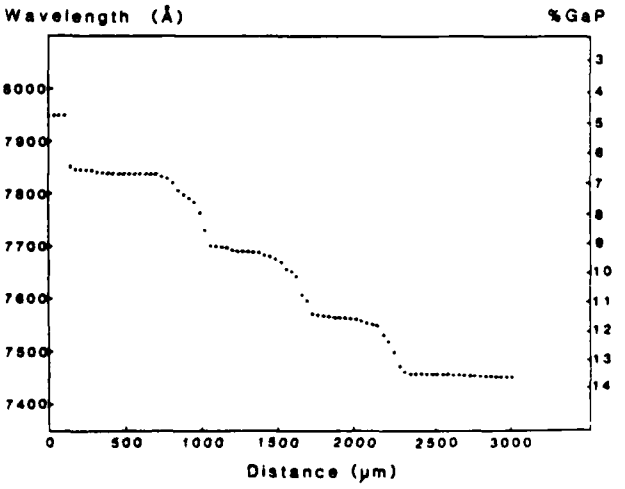

FIG. 4. Photoluminescence peak wavelength and percent GaP vs position across a substrate with five layers of selectively grown Ga(AsP).

broader and may be the result of signals originating from the two adjoining regions. The width of the regions where the PL wavelength changes between two constant values varies from 20 to about 150 μm as shown in Fig. 4. These values can be considered as the upper limits for the transition width between two adjacent selective growth regions since the laser beam has a finite size.

We have also used this selective growth technique to fabricate multiple color LED's on a single GaAs substrate. The emission spectra peaked at 9100, 8400, and 8700 Å for low levels of current injection. LED structures were obtained by selectively growing p-n junctions in Ga(AsP) with different compositions and thus band gaps. For the present growth temperature, it was not possible to achieve a high enough Zn doping level for good ohmic contacts, especially for high GaP content. For this case, junctions were fabricated by Zn diffusion into n-type selectively grown layers. This was achieved in an evacuated ampoule containing $ZnAs_2$ heated to 600 °C for 3 h. Device fabrication used standard metallization and etching techniques.

The process of selective growth using a moving substrate relative to a fixed mask can be a promising approach to integrating several devices. However, we believe that there are several factors that have to be addressed before such an approach can be made to meet most of the desired requirements. Since the growth is carried out from sources in the gas phase, abrupt transitions in the lateral directions from one selective area to the next can be difficult to achieve. We have found that the thickness of the deposited layer is very small near the edge of the mask and then gradually approaches the desired thickness. The length of this taper depends, in part, on the thickness of the mask itself. This is a result of the inefficient process of supplying source molecules (TMG) and getting rid of reaction products (CH_4) close to the edge of the mask. This is especially true of a growth process that is controlled by mass transport mechanisms. Reducing the thickness of the mask can minimize such problems. For example, gradual variation over distances of several thousand microns, several hundred microns, and a few tens of microns for mask thicknesses of 200, 20, and 6 mils, respectively, was observed. We believe that even further reduction in the taper length can be achieved by using thinner masks. The thickness grading of deposited layers, however, can be beneficial in certain applications. For example, this tapered film can be used to couple light to another film with a different index of refraction.[8] Also, growth through an opening in a fairly thick mask will lead to a low growth rate near the walls of the mask and high growth rate in the center of the opening. This thickness variation will result in a curved surface which is desirable in some light-emitting devices.

The clearance between the mask and the substrate will allow gases to be trapped in such a gap. Thus growth may be present on parts of the substrate that are already masked. For a gap of few mils thick, we found that such an effect does not constitute any serious problems. Angle lapped samples (1/3°) for selected growth areas show that there was no growth in the masked regions. This might be a result of the fairly low mole fraction of the active molecules, such as TMG, in the carrier gas. For example, with a TMG flow rate of 10^{-5} mol/min in 500 cc/min of H_2 carrier gas, the trapped gases in a few mils thick gap will form less than a monolayer of GaAs in 1 min.

In conclusion, laterally selective growth has been successfully demonstrated using MOCVD. This was achieved by using a specially designed susceptor that allows the substrate to move with respect to a stationary GaAs mask. We have used this technique to selectively deposit $GaAs_{1-x}P_x$ on a single GaAs substrate with different values of x and to obtain multiple color LED's on a single GaAs substrate. This masking technique can also be used to obtain a tapered film light-wave coupler and also as a means to grow films with curved surfaces.

This work is supported by the Army Research Office and the Air Force Office of Scientific Research.

[1]O. Wada, S. Miura, M. Ito, T. Fujii, T. Sakurai, and S. Hiyamizu, Appl. Phys. Lett. 42, 380 (1983).
[2]F. K. Reinhart and R. A. Logan, Appl. Phys. Lett. 27, 532 (1975).
[3]Jun Shibata, Ichiro Nakao, Yoichi Sasai, Soichi Kimura, Nobuyasu Hase, and Hiroyuki Serizawa, Appl. Phys. Lett. 45, 191 (1984).
[4]R. M. Kolbas, J. Abrokwah, J. K. Carney, D. H. Bradshaw, B. R. Elmer, and J. R. Biard, Appl. Phys. Lett. 43, 821 (1983).
[5]W. T. Tsang and A. Y. Cho, Appl. Phys. Lett. 32, 491 (1978).
[6]A. Y. Cho and W. C. Ballamy, Appl. Phys. Lett. 46, 783 (1975).
[7]C. Ghosh and R. L. Layman, Appl. Phys. Lett. 45, 1229 (1984).
[8]P. K. Tien, Rev. Mod. Phys. 49, 361 (1977).

InAsSbBi and InSbBi: POTENTIAL MATERIAL SYSTEMS FOR INFRARED DETECTION

S. M. Bedair, T.P. Humphreys, P. K. Chaing, and T. Katsuyama

Electrical and Computer Engineering Department
North Carolina State University
Raleigh, North Carolina 27695-7911

ABSTRACT

$InSb_{1-x}$ Bi_x ($0.01 < x < 0.14$) and InAsSbBi quaternary alloys are attractive materials for the development of semiconductor infrared detectors covering the 8-14 μm range.

We report for the first time, MOCVD growth of $InSb_{1-x}$ Bi_x ($0.01 < x < 0.14$) and $InAs_{1-x-y}$ Sb_x Bi_y with $0.5 < x < 0.7$ and $0.01 < y < 0.04$ on both GaAs and InSb substrates using AsH_3, TMSb, TEI and TMBi. Electrical measurements of the undoped $InSb_{0.99}$ $Bi_{0.01}$ shows a background carrier concentration of approximately $10^{16}/cm^3$ and a room temperature mobility of 20,215 $cm^2/V.sec$. To-date, these are the best reported electrical measurements for this ternary alloy.

The formation of a secondary Bi phase and single crystal growth of metallic bismuth-antimony at the surface of In Sb_{1-x} Bi_x which results in deterioration of morphology with increasing values of x is also investigated. A wide range of analytic techniques, including SEM, EDX, electron microprobe and AES have been employed in our surface analysis.

Introduction

This paper reports the first results on the epitaxially growth of thin film $InSb_{1-x}$ Bi_x ($0.01 < x < 0.14$) and $InAS_{1-x-y}$ Sb_x Bi_y with $0.5 < x < 0.7$ and $0.01 < y < 0.04$ semiconducting alloys by MOCVD.

Present results include growth parameters, electrical, and crystal characterizations. Surface derived features for $InSb_{1-x}Bi_x$ were also investigated by SEM (scanning electron microscopy) with supplemental element identifications by EDX (energy dispersive X-ray analysis), electron microprobe analysis and AES (Auger electron spectroscopy).

Results and Discussion

Epitaxial layers were grown in a vertical quartz reactor operating at atmospheric pressure. Arsine (AsH_3), Triethylindium (TEI) (Alfa), trimethylantimony (TMSb) (Alfa) and trimethylbismuth (TMBi) (Alfa) were used as arsenic indium, antimony and bismuth sources, respectively. The TMBi bubbler was maintained at approximately -12°C, thus keeping the partial pressure of the TMBi vapor in the gas phase low enough to deposit a few percent of Bi in the solid phase. Epilayers were grown on both (100) InSb and Cr doped semi-insulating GaAs at a growth temperature of 445°C.

Compiled in Table 1 is a summary of the growth parameters, solid composition, carrier concentration and carrier mobility for several $InSb_{1-x}Bi_x$ and InAsSbBi samples. In the absence of a high resistivity InSb substrate all Hall measurements were conducted on $InSb_{1-x}Bi_x$ and InAsSbBi epilayers deposited on semi-insulating (100) GaAs. All grown $InSb_{1-x}Bi_x$ epilayers were n-type with carrier concentrations in the low $10^{16}/cm^3$ to the $10^{17}/cm^3$ range. The same range of carrier concentration was also observed for the deposition of epilayers of InSb under similar conditions (without Bi doping). In particular, it is clear that the addition of a few percent of Bi to the InSb solid film does not result in a significant change in the carrier concentration. A dramatic improvement however is observed in the electron mobility, even in cases were the solubility limit of Bi is

exceeded. For instance, the epilayer $InSb_{0.86}$ $B_{0.14}$ has a electron mobility which is approximately twice the mobility of a InSb film (5000 cm^2/V sec) grown under similar conditions. (Table 1) Epilayer thickness for both InSb and $InSb_{1-x}$ Bi_x corresponding to sample runs 229, 231 and 233 was approximately 1 μm. When thicker layers of $InSb_{1-x}$ Bi_x were deposited 2 μm (run #253), a electron mobility of 20,215 cm^2/V.sec was recorded at room temperature. The corresponding mobility at 77K was 6800 cm^2/V.sec. This decrease in mobility at low temperature is attributed to the predominance of a Dexter-Seitz's dislocation scattering mechanism. Further, it is noted that the mobility of this material is far superior to that grown by existing MBE techniques. For instance, with a comparable Bi concentration in the solid, carrier concentrations and mobilities grown by MBE are 1.6 x $10^{18}/cm^3$ and 480 cm^2/V.sec, respectively [1,2]. This may be compared to 4 x $10^{16}/cm^3$ and 20,215 cm^2/V.sec in the present study.

Also compiled in Table 1 are the electrical characteristics of the InAsSbBi alloys. Carrier concentrations of the grown films are in the high $10^{16}/cm^3$ to low $10^{17}/cm^3$ range. The incorporation of Bi in InAsSb, although improving the mobility slightly, resulted in a significant degradation of surface morphology.

The surface morphology and microstructure of the $InSb_{1-x}$ Bi epilayers corresponding to a InBi mole fraction of 3% (run #233) and 12% (run #229) are shown in Figure 1 (a) and (b), respectively. Three regions are clearly defined on both SEM micrographs. Region A, we identify as polycrystalline coherent precipitates. They have a regular geometry, both square and oblong in appearance, and are randomly distributed over the surface. The corresponding distribution surface density is largest on the $InSb_{1-x}$ Bi_x epilayer for x = 14.5 (run #239) and is reduced to very low levels with

decreasing x. The precipitates are small, ranging from 1 μm to 5 μm. Dimensions perpendicular to the surface are of the order of 1000 Å, as determined by Ar^+ ion milling and alpha step measurements. Orthorhombic single crystal formation with prefered surface orientation is clearly illustrated in region B. Dimensions of these single crystals are large, varying in length from 5 μm to 10 μm. Surface distribution density is largest for the $InSb_{1-x}Bi_x$ (x = 14%) epilayer and as x is reduced below the bulk solubility limit [3,4], the features completely disappear. Region C represents an intermediate area between the polycrystalline phase and single crystal structures that is both featureless and smooth.

Examination of the various surface regions by EDX gives several interesting results (Figure 2). For instance, Region A is mainly composed of Bi precipitates segregated at or near the surface. Indium is also incorporated in this polycrystalline precipitate as confirmed by electron microprobe analysis. Furthermore, employing glacing angle x-ray diffraction confirms the presence of polycrystalline phases of InBi and In_2Bi together with metallic Bi [1,2]. Region B has been identified as single crystal (metal-alloy) BiSb, that is formed during growth due to an excess of free antimony at the surface. Auger analysis confirms the presence of a Sb rich surface in all of the $InSb_{1-x}Bi_x$ epitaxial grown films. Coalescence of free Bi and Sb on the surface to form single crystal BiSb on cooling is tentatively proposed. The smooth mirror-like surface pertaining Region C is depleted of Bi and appears to be composed only of InSb.

In the case of $InSb_{1-x}Bi_x$ (x=0.01) whose InBi % composition is below the solubility limit of 2.6% in InSb [3,4], the surface morphology was good with only a small surface density of second phase polycrystalline Bi precipitates.

In conclusion, we have successfully grown InAsSbBi quaternary and $InSb_{1-x}Bi_x$ epilayers over a wide range of x values. High electron mobilities have been recorded for these $InSbi_{1-x}Bi_x$ films grown below the InBi% solubility limit. A trend reflecting the deterioration in surface morphology with increasing x has been observed. Investigation of the corresponding surface microstructure reveals the predominance of polycrystalline phases of In_2Bi, InBi and metallic Bi. The presence of metallic alloy BiSb is also observed on those films were the InBi% exceed the solubility limit.

References

1. A. J. Noreika, J. Greggi, Jr., W. J. Takei and M. H. Francombe, J. Vac. Sci. Technol. A1, 558 (1983).

2. B. Joukoff and A. M. Jean-Louis, J. Cryst. Growth. 12, 169 (1972).

3. J. L. Zilko and J. E. Green, Appl. Phys. Lett. 33, 256 (1978).

4. A. J. Noreika, W. J. Takei, M. H. Francombe and C. E. C. Wood, J. Appl. Phys. 53, 4932 (1978).

RUN	Growth Temperature (°C)	Epilayer Thickness (μm)	Gas Phase Composition (μ mol./min)				Solid Composition		Carrier Concentration n (cm^{-3}) [300K]	Mobility μ (cm^2/V.sec) [300K]
			TEI	TMSb	AsH_3	TMBi	InSb%	InBi%		
228	445	1	80	8	-	-	-	-	3×10^{16}	5000
229	445	1	80	8	-	1.2	-	12	1×10^{17}	5000
231	445	1	80	8	-	2.4	-	14.5	2×10^{17}	10,940
233	445	1	80	8	-	0.5	-	3	7×10^{16}	4000
253	445	2	80	8	-	0.3	-	<1	4×10^{16}	20,215
235	445	1	130	16	5.5	1.2	52	4.4	6×10^{16}	6000
236	445	1	160	20	5	1.2	52	1	2×10^{17}	8000

TABLE 1 Growth conditions and electrical Hall measurements for $InSb_{1-x}Bi_x$ and InSbAsBi

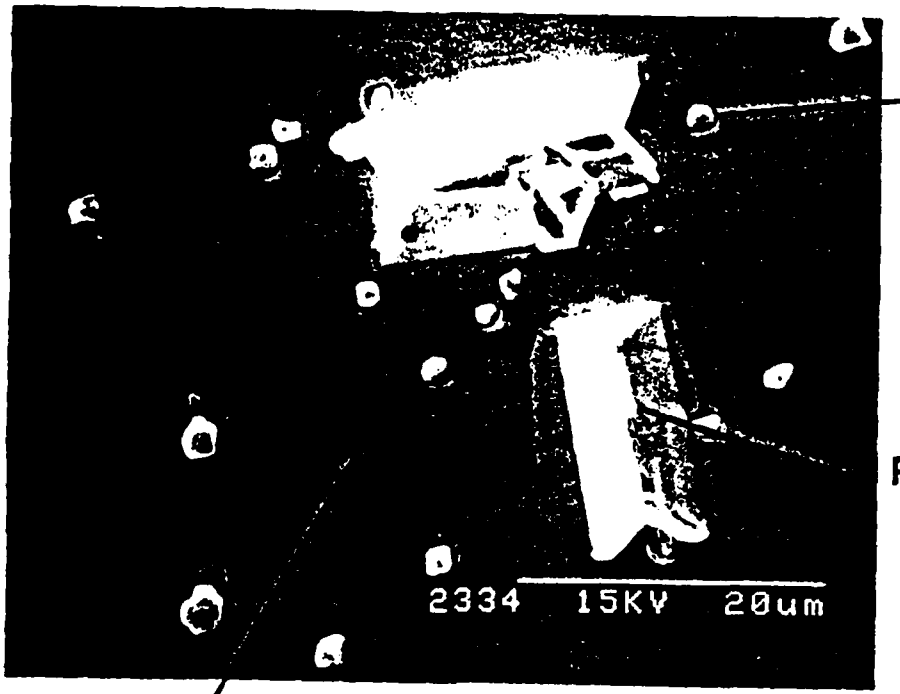

(a) $InSb_{0.97}Bi_{0.03}$

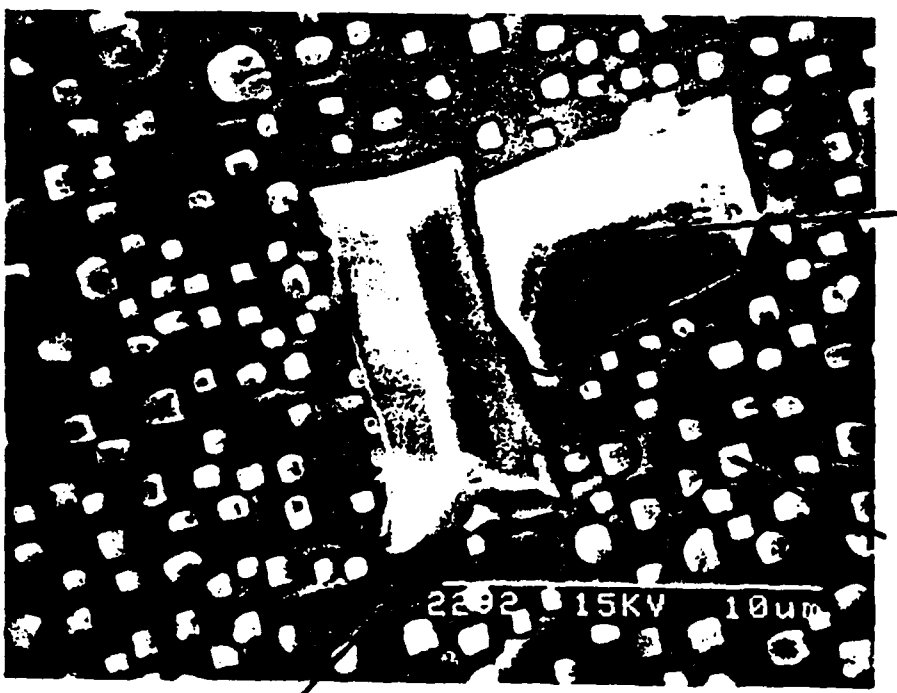

(b) $InSb_{0.88}Bi_{0.12}$

Figure 1.

SEM micrographs of $InSb_{1-x}Bi_{x}$ films were (a) x=0.03 (b) x=0.12 of 1μm thickness grown on a (100) orientated InSb substrate.

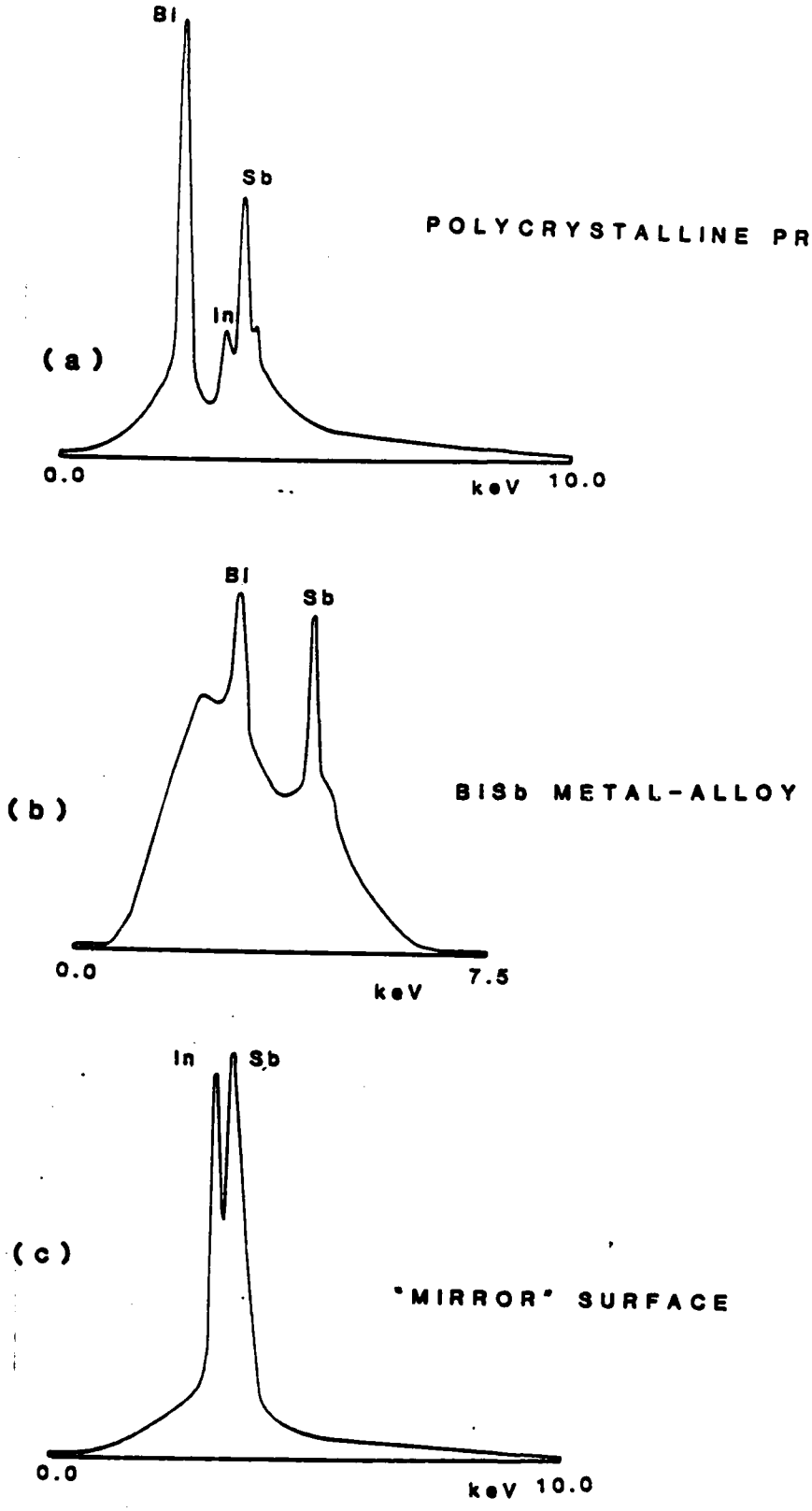

Figure 2

Energy dispersive X-ray (EDX) traces corresponding to (a) Region A (b) Region B and (c) Region C in Figure 1.

Reprinted from JOURNAL OF THE ELECTROCHEMICAL SOCIETY
Vol. 131, No. 10, October 1984
Printed in U.S.A.

Growth of InSb and $InAs_{1-x}Sb_x$ by OM-CVD

P. K. Chiang and S. M. Bedair

Department of Electrical and Computer Engineering, North Carolina State University, Raleigh, North Carolina 27695-7911

ABSTRACT

Organometallic chemical vapor deposition (OM-CVD) growth of InSb and $InAs_{1-x}Sb_x$ has been obtained using triethylindium (TEI), trimethylantimony (TMS), and arsine (AsH_3) on (100) GaAs, (100) InSb, and (111)-B InSb substrates. InSb with excellent morphology was achieved on both (100) InSb and (111)-B InSb substrates. The measured electron mobility at 300 K of undoped InSb grown on (100) GaAs semi-insulating substrates was 40,000 $cm^2/V\text{-}s$ at a carrier concentration of $N_D\text{-}N_A = 2.0 \times 10^{16}\ cm^{-3}$. Carrier concentration of $N_D\text{-}N_A = 1.2 \times 10^{15}\ cm^{-3}$ has been measured at 77 K. $InAs_{1-x}Sb_x$ ($0.07 \leq x \leq 0.75$) with mirror-like surfaces have been grown on (100) InSb and InAs substrates. This composition range of $0.55 < x < 0.75$ (Eg = 0.1 eV) has been successfully achieved for the first time. Solid composition variations as a function of growth temperature and InSb substrate orientations are also discussed.

There are two wavelength ranges, 3-5 and 8-12 μm, which cover the atmosphere window where minimum absorption is present. The InSb infrared detector has significant application for the detection of 3-5 μm radiation. This material has received increasing attention over the past few years. Epitaxial growth of InSb has been reported by LPE (1); however, there are several problems associated with the surface morphology. MBE growth of InSb (2) has been also recently reported; however, the electrical properties of the epitaxial layers have not been reported. Organometallic chemical vapor deposition (OM-CVD) is a potential technique for the epitaxial growth of InSb on large area substrates with surface morphology and electrical properties suitable for infrared focal plane arrays. Relatively little work has been reported on the growth of InSb and its alloys by OM-CVD. Manasevit (3) reported the growth of InSb on Al_2O_3 by OM-CVD with a room temperature mobility of 15,000 $cm^2/V\text{-}s$ and a carrier concentration of $(2\text{-}3) \times 10^{18}\ cm^{-3}$; however, no discussion of optimized growth parameters and the growth of epitaxial layers on InSb substrates has yet been reported.

$InAs_{1-x}Sb_x$ with $x = 0.6$ has the lowest bandgap (= 0.1 eV) of the III-V compounds. This bandgap can be suitable for detectors in the 8-12 μm wavelength region. $InAs_{1-x}Sb_x$ epilayer growth by LPE is difficult because of the very wide separation of liquidus and solidus curves in the phase diagram (4). There have been several reports of OM-CVD growth of $InAs_{1-x}Sb_x$ on InAs and insulating substrates (5, 6); however, poor surface morphology of the epitaxial layers has always been a problem especially for high value of x. We are not aware of any reported epitaxial growth of $InAs_{1-x}Sb_x$, with $0.5 < x < 0.7$, where the bandgap is about 0.1 eV.

In this paper, we report for the first time the epitaxial growth of InSb on InSb substrate by OM-CVD. Optimum growth conditions for mirror-like surfaces and the electrical properties of the epitaxial layers will be presented. Also, we report here the growth of $InAs_{1-x}Sb_x$ on InSb and InAs substrates with mirror-like surfaces over the composition range $0 < x \leq 0.75$.

Experimental

Epitaxial layers were grown in a vertical quartz reactor (9.5 cm id and 30 cm long) using 300 kHz RF induction for heating the graphite susceptor. Triethylindium (TEI) (Alfa), trimethylantimony (TMS) (Alfa), and arsine (AsH_3) (5% in H_2, Mathoson or Phoenix Research) were used as indium, antimony, and arsenic sources, respectively. Palladium-diffused H_2 was used as the carrier gas at a nominal flow rate of 3.6 l/min. Substrates included (100), (111)-B InSb, and (100) 2° toward [110] InAs and Cr-doped semi-insulating GaAs.

Both InSb and GaAs substrates were prepared by cleaning with TCE, acetone, and methanol. Final treatments included an 8:1 (lactic acid:HNO_3) etching for InSb, and a 7:1:1 (H_2SO_4:H_2O_2:H_2O) etching for GaAs substrates.

The deposition temperature for InSb was varied from 375° to 480°C. Both TEI and TMS flows were started when the substrate temperature reached the growth temperature for InSb deposition. No group V overpressure was maintained during the preheat.

$InAs_{1-x}Sb_x$ growth on (100) InSb substrates showed mirror-like surface morphology with different III/V ratios. However, it had not shown satisfactory surface morphology on (111)-B InSb substrates; therefore, we concentrated our experiments on (100) InSb substrates.

Conventional van der Pauw method on clover leaf samples cut from the epitaxial layers grown on Cr-doped GaAs substrates was used with alloyed In contacts for the electrical characterization. X-ray diffraction was used for determining the solid composition of InSb in $InAs_{1-x}Sb_x$.

Results and Discussion

InSb.—The optimum growth conditions which produced the best surface morphology on both (100) and (111)-B InSb substrates are 460°C growth temperature with flow rates of 1.45×10^{-5} mol/min and 1.13×10^{-5} mol/min for TEI and TMS, respectively. Figure 1 shows the surface morphologies of InSb epi-layers grown on (100)- and (111)-B InSb substrates under optimum growth conditions. The best results were obtained with a slightly In-rich gas phase (TMS/TEI = 0.78 partial pressure ratio) similar to the OM-CVD growth of GaSb under Ga-rich gas phase done by Cooper *et al.* (7). This is different from most arsenic containing growth, such as GaAs, which are grown with a group V-rich gas phase. It is more difficult to grow GaAs because excess As is very volatile at the growth temperature for GaAs; therefore, it is easily separated from the binary during growth (8). However, In and Sb have a relatively low vapor pressure at growth temperatures less than 480°C. Excess In or Sb will deposit on the substrate and incorporate into the layer as In or Sb droplets.

Figure 2 shows that the growth rate is proportional to the TMS flow rate with a constant TEI flow rate and growth temperature. Growth rate varies from 0.01 to 0.043 μm/min while maintaining good surface morphology.

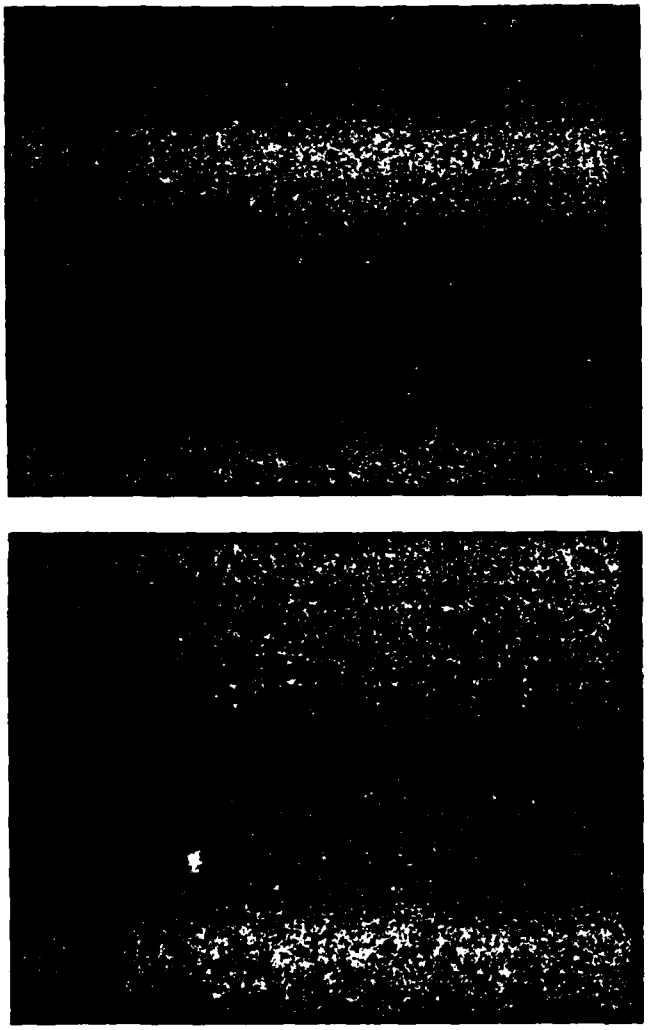

Fig. 1. Surface morphologies of InSb epilayers grown on two InSb substrate orientations. a (top): (100) InSb substrate (300×). b (bottom): (111)-B InSb substrate (300×).

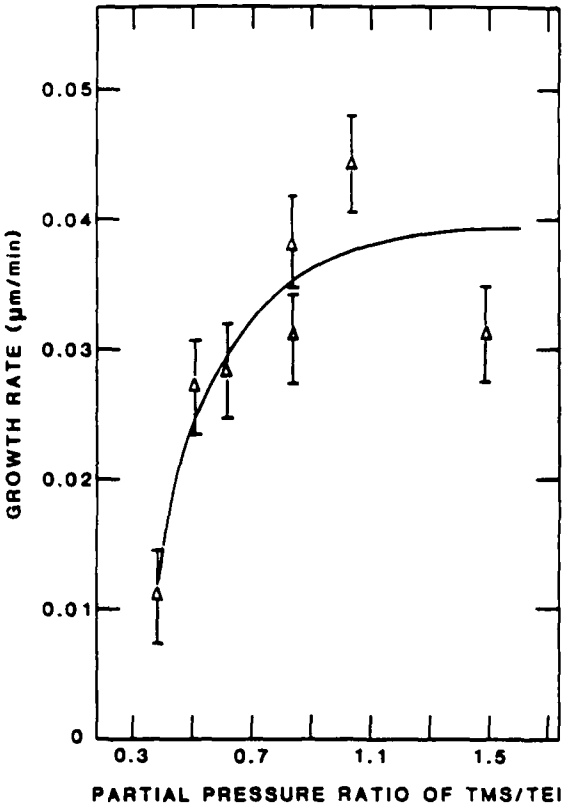

Fig. 2. Growth rate of InSb as a function of partial pressure ratio of TMS/TEI with TEI = 2.90×10^{-5} mol/min and growth temperature 450°C.

This growth rate of 2.5 μm/h makes OM-CVD a very practical method for the epitaxial growth of InSb.

The dependence of growth rate on growth temperature with constant TMS/TEI partial pressure ratio is shown in Fig. 3. Both higher growth rate and better surface morphology have been obtained at a high growth temperature. At growth temperatures above 480°C, local melting of the InSb substrate was observed (InSb mp = 525°C). In addition, there was no growth when temperature was decreased to 375°C, probably owing to the insufficient dissociation of the OM sources. Because of the lack of available InSb semi-insulating substrates, we used GaAs (100) 2° toward [110] Cr-doped semi-insulating substrates to study the electrical properties of the InSb epilayer. It could be estimated (9) that there exists 10^{14} cm^{-2} dislocation density at the interface between the InSb epilayer and the (100) GaAs substrate due to their 14% lattice mismatch. The InSb epilayers grown on GaAs were shown to be single crystal by x-ray diffraction, however, with poor surface morphology. Figure 4 shows the room temperature electron mobility *vs.* the partial pressure ratio of TMS/TEI with constant TEI flow rate at two different growth temperatures. All samples show n-type conductivity at partial pressure ratios of TMS/TEI from 0.4 to 1.5. At room temperature, carrier concentrations in the range 2×10^{16} to 8×10^{16} cm^{-3} have been obtained. This range is close to what can be achieved since at room temperature the intrinsic carrier concentrations for InSb, n_i, is about 2×10^{16} cm^{-3}. At liquid nitrogen temperature, the lowest measured carrier concentration is about 1×10^{15} cm^{-3}. This indicates the presence of N_D-N_A background impurity of the order of magnitude 10^{15} cm^{-3} since n_i for InSb at liquid nitrogen temperature is in the 10^9 cm^{-3} range. We have not yet identified the nature and sources of these impurities.

Our best room temperature electron mobility is 40,000 cm^2/V-s at a carrier concentration of N_D-N_A = 2.0×10^{16} cm^{-3} (thickness = 1 μm) grown at 400°C with a 2.9×10^{-5} and 2.47×10^{-5} mol/min flow rate of TEI and TMS, respectively. This result is comparable with what has been

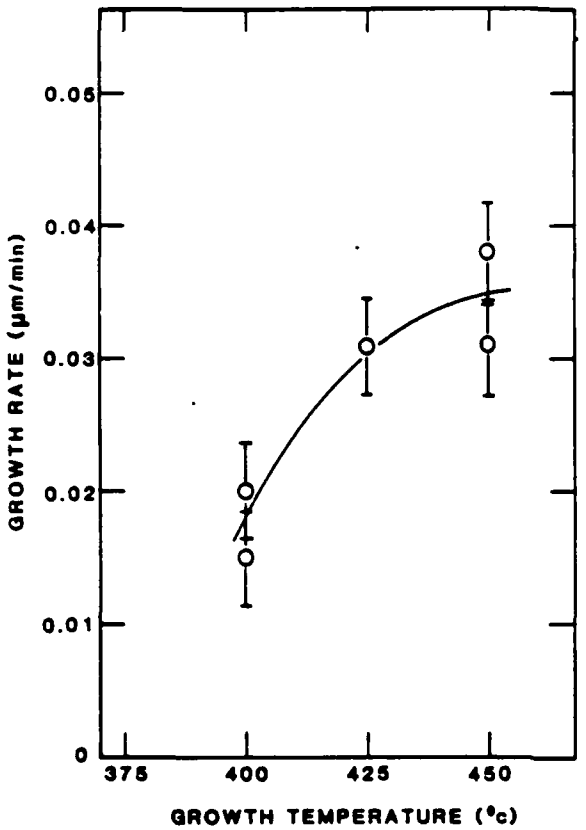

Fig. 3. Growth rate of InSb as a function of temperature with flow rate of TEI:TMS = 2.9×10^{-5}:2.47×10^{-5} mol/min.

obtained using infinite solution liquid-phase epitaxy by Holmes and Kamath (1). They reported electron carrier concentrations and mobilities for 20 μm thick InSb epilayers ranging from 2 to 4×10^{16} cm^{-3} and from 5 to 6 $\times 10^4$ cm^2/V-s, respectively. In Fig. 4, we also find that the electron mobilities increase from 25,000 cm^2/V-s for a 2 μm thick epilayer to 35,000 cm^2/V-s for a 4 μm thick epilayer, which were grown at the same growth conditions. This indicated that mobility is dependent on the thickness of the epilayer as has been previously observed in the OM-CVD growth of GaAs (10). Figure 5 shows the temperature dependence of the electron mobility. The electron mobility tends towards a maximum value in the vicinity of 300 K and decreases monotonically with increasing temperature. This result is similar to that reported by Wieder's study of dendritic films of InSb (11). Such mobility temperature dependence can be partially explained to be a result of the presence of high dislocation density in the InSb epilayer on GaAs substrates. Ehrenreich (12) has shown that lattice scattering dominates above 200 K and has a temperature dependence of the electron mobility $\mu \alpha T^{-1.7}$. In addition, Dexter and Seitz (13) have indicated that the density of dislocations, N, necessary to give dislocation scattering at temperature T equal to the lattice scattering is $N = 6 \times 10^4 T^{3/2}$ cm^{-2} which is $\approx 10^{11}$ cm^{-2} at 300 K. Since there exists 10^{14} cm^{-2} dislocation density at the interface between InSb epilayer and (100) GaAs substrate, dislocation scattering has to be considered as well as impurity and lattice scattering effects. Dexter and Seitz also indicated that dislocation scattering effect increases with decreasing temperature. The reciprocal mobility can be described as

$$\frac{1}{\mu} = \frac{1}{\mu_l} + \frac{1}{\mu_i} + \frac{1}{\mu_d} \qquad [1]$$

where μ, μ_l, μ_i, and μ_d represent the experimentally measured mobility, impurity scattering mobility, lattice scattering mobility, and dislocation scattering mobility, respectively. From Putley's paper (14), we estimated that the impurity scattering mobility, at carrier concentration,

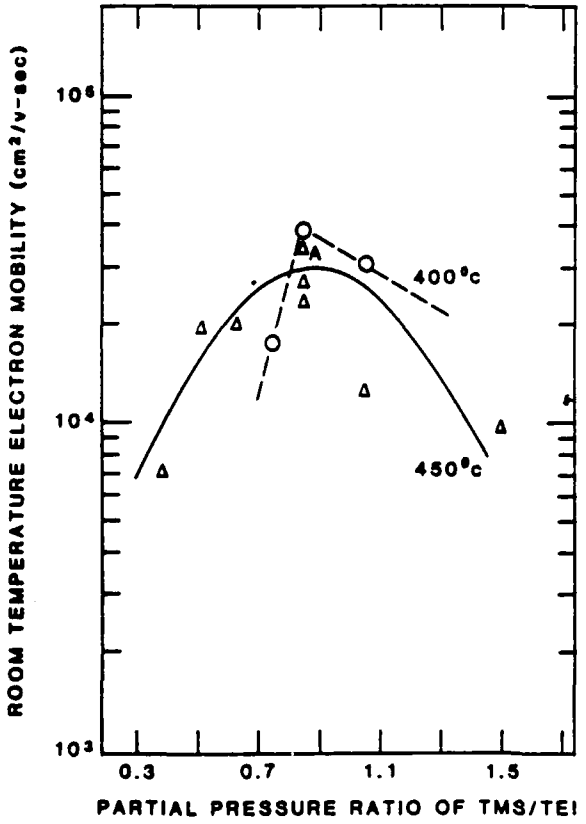

Fig. 4. Room temperature electron mobility of InSb as a function of TMS/TEI partial pressure ratio (flow rate of TEI fixed at 2.9×10^{-5} mol/min) at growth temperatures 400°C (○) and 450°C (△). The thickness of all the samples are 1-2 μm except sample A (≃ 4 μm). Substrates are (100) GaAs Cr-doped semi-insulators.

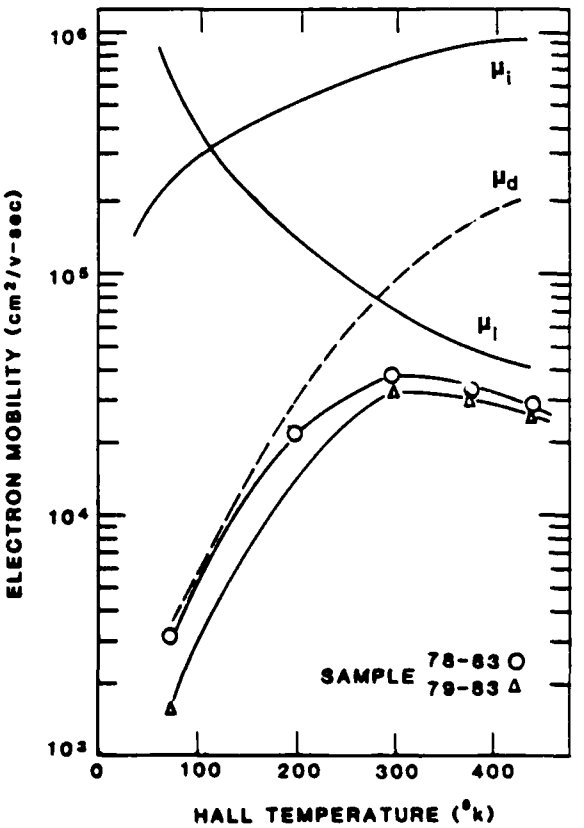

Fig. 5. Temperature dependence of the InSb electron mobility. The measured values of μ were used in conjunction with lattice scattering mobility μ_l and impurity scattering mobility μ_i to determine the dislocation scattering mobility μ_d.

$n = 10^{16}$ cm^{-3}, $\mu_1 \simeq 1.1 \times 10^4\ T^{0.73}$. For the two curves shown in Fig. 5, the measured values of μ were used in conjunction with $\mu_1 = 1.1 \times 10^4\ T^{0.73}$ and $\mu_1 = 1.09 \times 10^9\ T^{-1.68}$ (11) to determine μ_d as a function of temperature by means of Eq. [1]. The results indicate that μ_d increases linearly with temperature. Thus, Eq. [1] can be expressed as

$$\frac{1}{\mu} = \frac{T^{-0.73}}{1.1 \times 10^4} + \frac{T^{1.68}}{1.09 \times 10^9} + \frac{1}{\mu_d}$$

letting $\mu_d = \beta T$ where β is constant ($\simeq$ 330 cm^2/V-s/K).

This result shows that the Dexter-Seitz's dislocation scattering mechanism represents the mobility limiting process. Finally, we believe that much higher mobility can be achieved both at 77 and 300 K if InSb is grown on a lattice matched semi-insulator such as CdTe.

$InAs_{1-x}Sb_x$.—$InAs_{1-x}Sb_x$ ternary layers have been grown in the composition range of $0 < x \leq 0.75$ on (100) InSb substrates, with mirror-like surface morphologies. The variations of the solid composition at growth temperature of 460°C with constant TEI and AsH_3 flow rates is shown in Fig. 6. As shown in this figure, the mole percent of InSb in the solid phase cannot be increased substantially upon further increase in TMS flow rates. Values of x higher than 0.6 can be achieved by decreasing the mole fraction of AsH_3 in the gas phase. This has also been observed in the case of OM-CVD growth of $GaAs_{1-x}Sb_x$, where reducing the AsH_3 partial pressure was found to be more effective in obtaining higher GaSb in the solid phase than increasing the TMS partial pressure as being reported by Bedair *et al.* (15). Data shown in Fig. 6, however, are obtained for the minimum AsH_3 partial pressure that can be obtained from our OM-CVD system. Another way to increase the value of x is to decrease the growth temperature and to increase the TEI flow rate. Figure 7 shows the dependence of the InSb percent in the solid phase on the TEI flow rate at two different growth temperatures. As shown in this figure, growth at 440°C resulted in higher values of x than that at 460°C for the same flow rate of reacting gases. A possible explanation is that AsH_3 dissociates more efficiently at higher temperatures and As is preferentially incorporated into the crystal over Sb (7). Under this circumstance, lower InSb percent in the solid phase was obtained at higher temperatures. In this figure, we also show the dependence of the solid composition on the substrate orientations. With each substrate orientation, the InSb percent in solid phase is proportional to the flow rate of TEI. The growth on (111)-B InSb substrates has a higher percent of InSb in the solid composition as compared to the growth on (100) InSb substrates. This result may indicate that the growth is controlled by surface reaction kinetics rather than by mass transport.

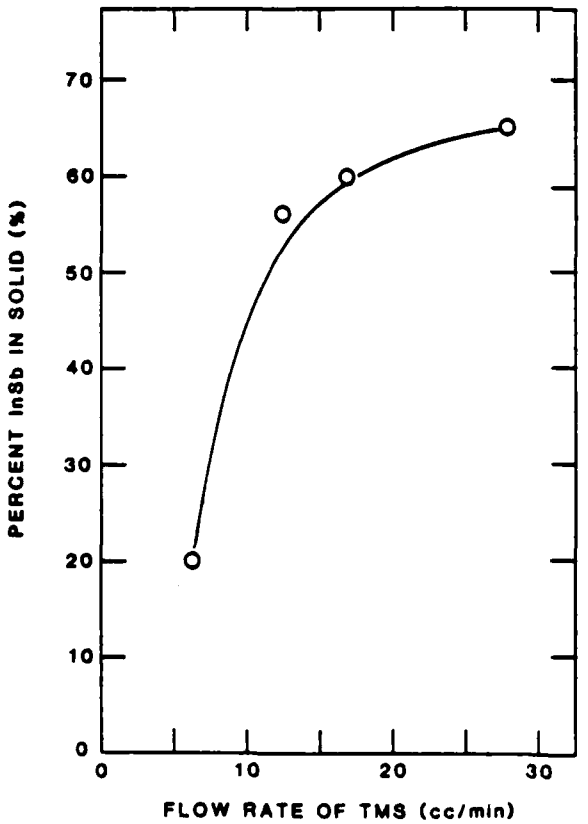

Fig. 6. Mole percent of InSb in the InAsSb epilayer as a function of the flow rate of TMS with the flow rate of TEI:AsH_3 = 2.03 × 10^{-5}:1.22 × 10^{-5} mol/min at growth temperature 460°C using (100) InSb substrates.

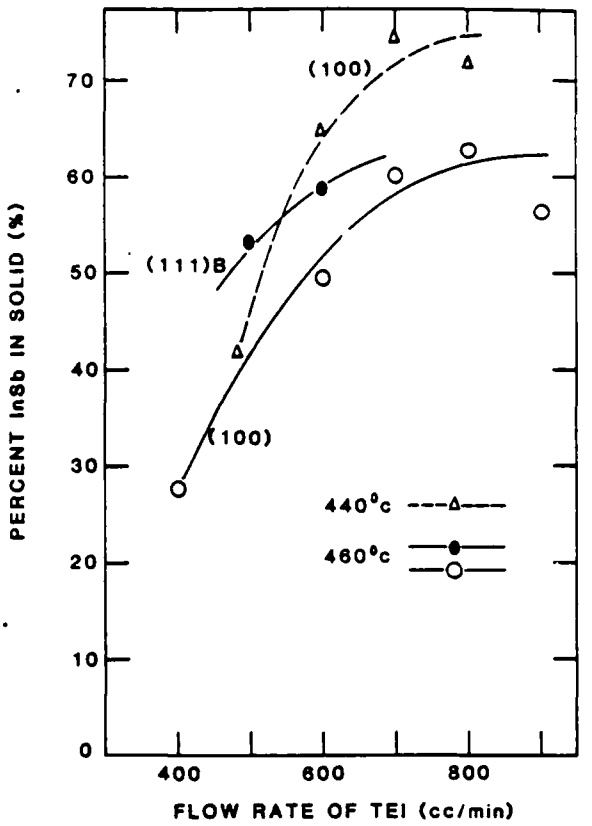

Fig. 7. Mole percent of InSb in the InAsSb epilayer as a function of the flow rate of TEI with the flow rate of TMS:AsH_3 = 2.96 × 10^{-5}: 1.22 × 10^{-5} mol/min at growth temperature 460°C using (100) InSb (-o-o-) and (111)-B InSb (-•-•-) substrates. This figure also shows the mole percent of InSb in the InAsSb epilayer as a function of the flow rate of TEI with the flow rate of TMS:AsH_3 = 2.96 × 10^{-5}:1.22 × 10^{-5} mol/min grown on (100) InSb substrates at two different growth temperatures, 460°C (-o-o-) and 440°C (-△-△-).

Finally, we had grown $InAs_{1-x}Sb_x$ with $x = 0.63$ on (100) 2° toward [110] InAs substrates at growth temperature 460°C with very good surface morphology. This InSb percentage in the solid is higher than what had been previously achieved on InAs substrates by OM-CVD (5, 6). However, further study of the growth on InAs substrates has not been done yet.

Conclusion

OM-CVD epitaxial growth of high quality InSb has been demonstrated. This was achieved by careful control of growth temperature and the TMS/TEI partial pressure ratio. A room temperature mobility of 40,000 cm^2/V-s has been measured even with 14% lattice mismatch between the InSb epilayer and GaAs substrate. Dislocation scattering mechanism has been used to explain the variations of mobility with temperature.

$InAs_{1-x}Sb_x$ growth on (100) InSb substrates has been obtained from 7% to 75% InSb in the solid phase with good surface morphologies. The dependence of the InSb percent in the solid phase on growth temperature and gas

partial pressures can be explained by preferential incorporation of As over Sb. In addition, the variation of the InSb percent in the solid phase as a function of substrate orientation was studied. Thus OM-CVD technique can be a potential technique of the epitaxial growth of InSb and $InAs_{1-x}Sb_x$ for infrared focal plane arrays covering the 3-5 and 8-12 μm ranges.

Acknowledgments

This work was supported by NASA and Army Office of Research. The authors would like to thank Dr. J. R. Hauser, R. Sillmon, T. Katsuyama, R. J. Markunas, Cherie Winston, and J. H. Wang for their fruitful discussions and help.

Manuscript submitted Nov. 17, 1983; revised manuscript received May 29, 1984.

North Carolina University assisted in meeting the publication costs of this article.

REFERENCES

1. D. E. Holmes and G. S. Kamath, *J. Electron. Mater.*, **9**, 95 (1980).
2. A. J. Noreika, M. H. Francombe, and C. E. C. Wood, *J. Appl. Phys.*, **52**, 7416 (1981).
3. H. M. Manasevit, *J. Cryst. Growth*, **55**, 1 (1981).
4. G. B. Stringfellow and P. E. Greene, *This Journal*, **118**, 805 (1971).
5. T. Fukui and Y. Horikoshi, *Jpn. J. Appl. Phys.*, **19**, L53 (1980).
6. G. Nataf and C. Verie, *J. Cryst. Growth*, **55**, 87 (1981).
7. C. B. Cooper III, R. R. Saxema, and M. J. Ludowise, *Electron. Mater.*, **11**, 1001 (1982).
8. H. M. Manasevit and K. L. Hess, *This Journal*, **126**, 2031 (1979).
9. D. B. Holt, *J. Phys. Chem. Solids*, **27**, 1053 (1966).
10. P. D. Dapkus, H. M. Manasevit, and K. L. Hess, *J. Cryst. Growth*, **55**, 10 (1981).
11. H. H. Wieder, *Solid State Electron.*, **9**, 373 (1966).
12. H. J. Ehrenreich, *Phys. Chem. Solids*, **2**, 131 (1957).
13. D. L. Dexter and F. Seitz, *Phys. Rev.*, **86**, 964 (1952).
14. E. H. Putley, *Proc. Phys. Soc.*, **73**, 280 (1959).
15. S. M. Bedair, M. L. Timmons, P. K. Chiang, L. Simpson, and J. R. Hauser, *J. Electron. Mater.*, **12**, 959 (1983).

Journal of Crystal Growth 68 (1984) 477–482
North-Holland, Amsterdam

GaAsP–GaInAsSb SUPERLATTICES: A NEW STRUCTURE FOR ELECTRONIC DEVICES

S.M. BEDAIR, T. KATSUYAMA, P.K. CHIANG, N.A. EL-MASRY, M. TISCHLER and M. TIMMONS

Electrical and Computer Engineering Department, North Carolina State University, Raleigh, North Carolina 27695-7911, USA

OMCVD has been used to grow $GaAs_{1-z}P_z$–$Ga_{1-x}In_xAs$, $GaAs_{1-z}$–P_z–$GaAs_{1-y}Sb_y$, and $GaAs_{1-z}P_z$–$Ga_{1-x}In_xAs_{1-y}Sb_y$ superlattices (SL) in the composition range $0 < x < 0.25$, $0 < y < 0.3$ and $0 < z < 0.5$. Growth parameters for the synthesis of these new structures are reported. Superlattice structures are characterized by X-ray diffraction, photoluminescence and electron microprobe. Light-emitting diodes (LED's), based on these superlattices have been fabricated. We also report the synthesis of the first GaInPAsSb quinary alloy obtained by disordering this new SL. This new structure can be grown lattice-matched to a GaAs substrate and thus have potential applications in several electronic devices such as HEMT, LED and high speed detectors.

1. Introduction

Advances in electronic devices usually rely on progress achieved in the synthesis of new material systems and new structures. The superlattice (SL) is one of the newly developed structures that has both fundamental and technical interest. Most of the superlattice structures that have been studied so far are made of two binary compounds, such as GaSb–InAs [1], or a binary and ternary compounds, such as GaAs–AlGaAs, GaAs–InGaAs [2,3], GaAs–GaAsP [4] and CdTe–HgCdTe [5]. However, superlattices made of two ternaries or a ternary and a quaternary compound offer more degrees of freedom and can have several advantages over the present structures. For example, this new class of superlattices can have a large band-edge discontinuity and the compositions of the superlattice layers can be adjusted so that the superlattice, as a whole, can be lattice-matched to a given substrate.

We have recently reported [6] the synthesis of $GaAs_{1-y}P_y$–$In_xGa_{1-x}As$ superlattice. In this structure, with $y \approx 2x$ and equal layer thicknesses, when grown directly on a GaAs substrate, the InGaAs layers will be under compression, whereas the GaAsP layers will be under tension and the lattice parameter of the SL layers will be equal to that of GaAs. The uniqueness of this SL structure is that it allows the growth of strained layers of InGaAs that are lattice-matched to the GaAs substrate, and with a bandgap that can cover the 0.7–1.4 eV range. This will, for the first time, allow the investigation of the electronic properties of this ternary, for $0 < x < 0.5$, without the interference of the high density of dislocations that is usually encountered in their growth directly on a GaAs substrate.

Another SL structure which can have the same potential as GaAsP–InGaAs is GaAsP–GaAsSb. It can also be grown lattice-matched to a GaAs substrate. This will again allow the study of several fundamental properties of the GaAsSb ternary compounds, free from substrate-induced lattice defects. Additional degrees of freedom can be achieved in SL's made of ternary–quaternary layers such as GaAsP–GaInAsSb. The quaternary allows the possibility of achieving lower bandgap energies than the ternary alloys, for the same lattice constant. This will lead to less strain in the quaternary superlattice layers for the desired low bandgap in the SL structure. Another advantage in using the quaternary alloy is that it can avoid certain growth problems. For example, in the case of organometallic chemical vapor deposition, rather than growing $Ga_{0.5}In_{0.5}As$ which can be fairly difficult due to the reaction between In compounds and AsH_3, the same lattice constant can be achieved by growing the quaternary $Ga_{0.75}In_{0.25}As_{0.75}Sb_{0.25}$. The quaternary alloy has a lower In content than the ternary, thus reducing the elimination reaction in the gas phase. We report the growth of GaInAsSb

0022-0248/84/$03.00

quaternary alloy and the synthesis of the GaAsP–GaAsSb and GaAsP–GaInAsSb superlattices. Light Emitting Diodes (LED's) based on this superlattice have been fabricated, emitting at 1 μm wavelength.

2. Experimental

The epitaxial layers were grown by OMCVD at atmospheric pressure in a vertical reactor. OM sources are trimethylgallium (TMGa), triethythyindium (TEI), and trimethyantimony and were kept at 0, 20, and 0 °C, respectively. AsH_3 and PH_3, both 5% in H_2, were used as the As and P sources. Palladium diffused H_2 flowing at a rate of 3 to 4 l/min served as the carrier gas. Growth temperature was varied from 580 to 650 °C. The substrates were (100)GaAs oriented 2° toward the [110] direction. Epitaxial layers and superlattice structures were examined by X-ray diffraction. A standard scanning 2θ diffractometer study, using Cu Kα radiation was employed. Photoluminescence, electron microprobe analysis (EMP) and optical microscopic examinations were also used to examine the grown layers.

3. OMCVD growth of $Ga_{1-x}In_xAs_{1-y}Sb_y$

The growth of $Ga_{1-x}In_xAs_{1-y}Sb_y$ by OMCVD relies on our previous experiences in the growth of the InGaAs [7], GaAsSb [8], and InAsSb [9] ternaries. In order to minimize the parasitic reaction between AsH_3 and TEI, the mole fraction of TEI in the gas phase is adjusted such that the In composition in the solid phase, x, should be less than about 0.25. The incorporation of Sb in the OMCVD growth process is different from the incorporation of other column V elements such as P and As. This is because Sb has a relatively low vapor pressure at the growth temperature and excess Sb will be incorporated in the solid phase. In order to attain high values of GaSb or InSb in the growth of GaAsSb or InAsSb, it was found that it is more effective to decrease the AsH_3 partial pressure than to increase the TMSb partial pressure [8,9]. We have successfully grown $GaAs_{1-y}Sb_y$ and $InAs_{1-y}Sb_y$ with y as high as 0.7 and 0.8, respectively [8,9].

We have also found that the growth rate of GaAsSb [8], especially for high Sb concentrations in the solid phase, is not completely dependent on the TMGa mole fraction in the gas phase as is the case for GaAsP and AlGaAs. Lower growth rates have always been observed and were found to be correlated to the AsH_3 mole fraction in the gas phase even at growth temperatures higher than 600 °C. This has been previously explained [8] by assuming that the growth rate is the sum of the growth rates of the GaAs and GaSb sublattices. The growth rates in these two sublattices are controlled by the AsH_3 and the TMSb partial pressures.

Table 1 shows examples of the growth conditions and solid compositions for several GaInAsSb quaternary alloys. The solid compositions, lattice constant and bandgap are determined from EMP, X-ray diffraction and room temperature photoluminescence. To the best of our knowledge, this is the first reported epitaxial growth of this quaternary alloy over this range of compositions. These experimental results are in agreement with the predicted values of the lattice constant and

Table 1
Growth conditions for the $Ga_{1-x}In_xAs_{1-y}Sb_y$ quaternary alloy

Run	Growth temperature (°C)	Gas phase composition (μmol/min)				Solid composition		Lattice constant (Å)	Band gap (eV)
		TMG	TEI	AsH_3	TMSb	x	y		
115	570	20	4.4	48	106	25	20	5.818	0.85 [a]
116	600	20	3.3	96	71	17.5	4.4	5.732	1.18
117	600	20	5.5	69	106	11	5	5.731	1.2

[a] Calculated.

bandgap energy previously reported [10]. As shown in table 1 it is possible to obtain, using this quaternary alloy, epilayers with Eg = 0.85 eV without facing the problem of parasitic reaction between TEI and AsH_3.

4. $GaAs_{1-z}P_z$–$Ga_{1-x}In_xAs_{1-y}Sb_y$ superlattice

The choice of growth temperature was critical in this study. The incorporation of P is low at low growth temperatures [11] whereas the incorporation of Sb increases for low growth temperatures. Growth temperatures in the range of 600– 630 °C were found to be a good compromise to incorporate the desired atomic fraction of Sb, In and P in the superlattice layers. In order to insure that the average lattice spacing of the SL structure equals that of the GaAs substrate, a series of calibration runs were performed to grow separate layers of GaAsP and GaInAsSb. The partial pressures in the gas phase were adjusted so that $a_{GaAs} - a_{GaAsP}$ in the ternary layer is about equal to $a_{GaInAsSb} - a_{GaAs}$ in the quaternary layer. Thus for equal layer thicknesses in the SL structure, tensile and compressive stresses are hopefully equal in the ternary and the quaternary thin layers, respectively. The growth rate of the ternary and quaternary compounds was deduced from the growth of thick epitaxial layers. Typical growth time ranges from 10 to 15 s for both the GaAsP and GaAsSb or GaInAsSb layers. The AsH_3 was kept on during the whole growth period. TMGa and PH_3 were switched on for the growth of GaAsP. This was followed by one minute of flushing. Then TMG, TEI and TMSb were switched on to grow the quanternary alloys. GaAsP–GaAsSb and GaAsP–GaInAsSb strained-layer superlattices consisting of 30 to 50 periods have been epitaxially grown on a GaAs substrate. The total thickness of the superlattice structure, obtained from optical examination on cleaved layers, was in the range of 1–1.5 μm. The corresponding thicknesses of the individual ternary or quaternary SL layers are in the range of 150–250 Å. The period of these superlattices has also been deduced from the position of the extra satellite peaks [12] observed in the X-ray diffraction pattern. In general, there is reasonably good agreement (~ 10%) between the SL periods obtained from X-ray diffraction and from the thickness of the cleaved layers. EMP was used to determine the composition of the superlattice layers. Assuming equal layer thicknesses in the SL structure, EMP will give the average composition of the elements in the SL structure. Thus, values obtained for the atomic fraction of In, Sb and P from the EMP are one half of that actually present in the SL layers.

Fig. 1 shows the X-ray diffraction pattern of $GaAs_{0.76}P_{0.24}$–$Ga_{0.92}$ $In_{0.08}$ $As_{0.95}Sb_{0.05}$ SL made of 30 periods. The growth temperature is 630 °C and the growth time is 10 s for both the ternary and the quaternary alloy layers. The zero order diffraction, $n = 0$, gives the average lattice parameter of the SL and is closely matched to that of the GaAs substrate. The extra satellite peaks are due to the periodicity of the structure, giving a period

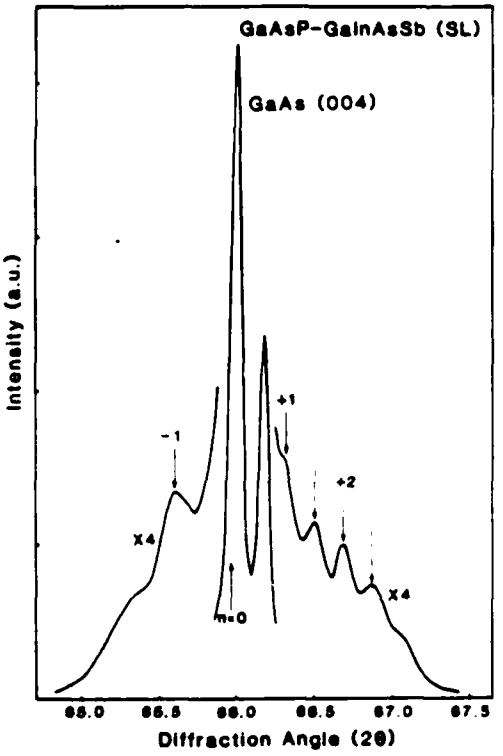

Fig. 1. X-ray diffraction pattern (400) of $GaAs_{0.76}P_{0.24}$–$Ga_{0.92}In_{0.08}As_{0.95}Sb_{0.05}$ SL. The n's show the order of the satellite peaks originating from the periodicity of the SL. Dotted arrows show Cu $K\alpha_2$ peaks.

of 300 Å which is consistent with the value obtained from the total thickness of the SL structure obtained on a cleaved sample.

Fig. 2 shows the X-ray diffraction pattern for a SL with an alloy composition which is comparable to that shown in fig. 1 for both the ternary and the quaternary alloys; however, the growth time per layer is doubled. The extra satellite peaks, in this case, are fairly intense and their intensity is comparable to that of the GaAs substrate. The period of this structure is about 630 Å as indicated from the position of the satellite peaks. These satellites seem to be modulating the diffraction patterns of two broad peaks centered around 65.25° and 66.8°. The position of these broad peaks are correlated to the composition of the quaternary layers (65.25°) and the ternary layers (66.8°). In this SL structure the thickness of the individual layers is

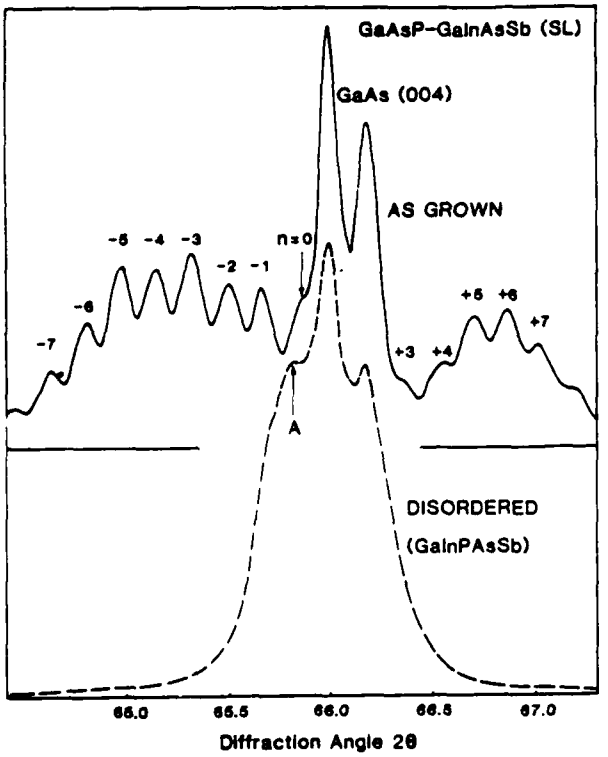

Fig. 2. X-ray diffraction pattern for fairly thick SL layers. The layers are of the same composition as that shown in fig. 1. Zn diffusion has resulted in disordering of this SL and thus forming the GaInAsSbP quinary alloy. The arrow A shows quinary peak.

greater then the critical thickness [4] h_c needed to relieve the strain present between the two layers. Thus part of this strain is relieved by the generation of dislocations. These dislocations are generated at the interfaces between the successive layers, and the broad peak can now results from the variation in the *d*-spacing of the individual SL layers. The presence of these dislocations at the interfaces manifests itself in the very poor photoluminescence characteristics of this SL. We feel that further work is needed to acquire more understanding of such behavior.

Zn diffusion [2] into the GaAsP–GaInAsSb SL structure has resulted in the complete disordering of the SL layers. For example, Zn diffusion in the GaAsP–GaInAs, GaAsP–GaAsSb and GaAsP–GaInAsSb superlattices resulted in the formation of GaInAsP, GaAsSbP quaternaries and the GaInAsSbP quinary alloy, respectively. Zn diffusion was accomplished via the standard closed-tube technique, where the SL, $ZnAs_2$ and InP were heated for 2 h at 800°C. X-ray diffraction in fig. 2 shows complete disorder of the SL, as indicated by the disappearance of the satellite peaks. The compositions of the homogeneous-disordered alloys were found to be in agreement with the values obtained from EMP. Detailed analysis of the variation of the lattice constant and bandgap with composition for the GaInAsSbP quinary alloy will be reported [13].

5. GaAsP–GaInAsSb light emitting diode

An LED structure is shown in figs. 3a and 3b where the active layer is made of a $GaAs_{0.8}P_{0.2}$–$In_{0.1}Ga_{0.9}As$ SL and a $GaAs_{0.76}P_{0.24}$–$Ga_{0.92}In_{0.08}As_{0.95}Sb_{0.05}$ Sl, respectively, DMZ and H_2Se have been used for p-type and n-type dopants, respectively. Doping levels are in the $10^{17}/cm^3$ range for both electrons and holes. A p^+-GaAs layer about 0.2 μm thick was grown on the Zn doped layers of the SL to facilitate the metallization process. This is made possible because the SL structure is closely matched to the GaAs substrate as shown in fig. 2. Device fabrication uses standard metallization and etching techniques. The emission spectra for these LED's is shown in fig. 4. Lifetime tests were

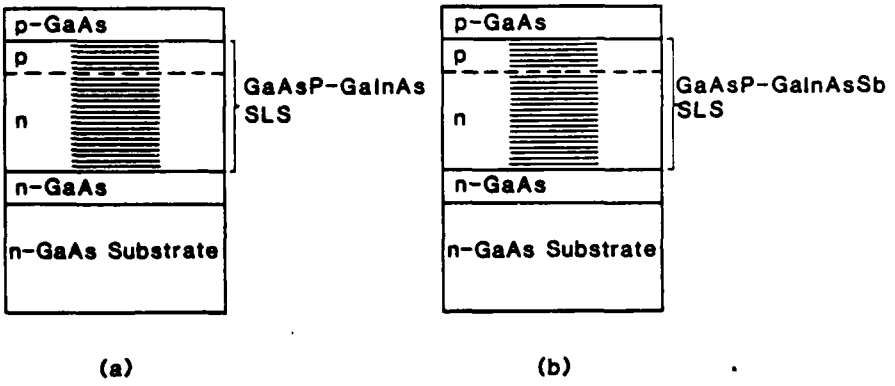

Fig. 3. Schematic of the LED structures: (a) $GaAs_{0.8}P_{0.2}$-$Ga_{0.9}In_{0.1}As$; (b) $GaAs_{0.76}P_{0.24}$-$Ga_{0.92}In_{0.08}As_{0.95}Sb_{0.05}$.

performed on GaAsP–InGaAs SL LED's at 25 °C, and several uncoated diodes were aged under constant injection levels of -20 A/cm^2 for over 200 h. We have not observed any degradation in the output emission intensity for such operation time. We have not yet done any lifetime testing on the GaAsP–InGaAsSb SL LED's.

The emission spectra in fig. 4b is fairly broad, which may be because the SL is not exactly matched to the GaAs substrate. This may also be due the interdiffusion across the interfaces between the ternary and quaternary alloys. Such interdiffusion can be enhanced by the presence of Sb atoms in this structure.

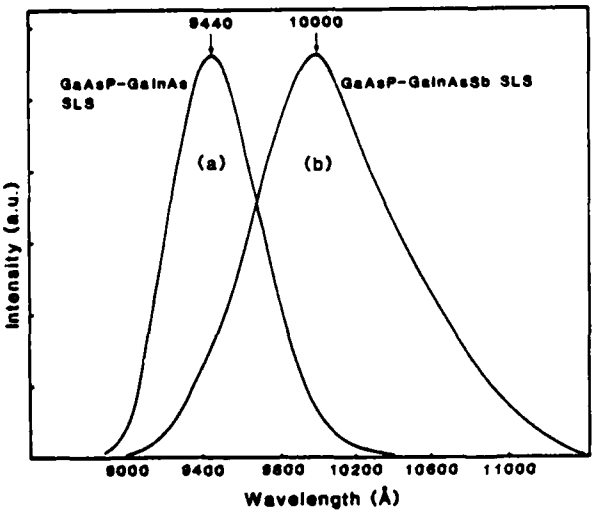

Fig. 4. Emission spectra: (a) for the structure shown in fig. 3a; (b) for the structure shown in fig. 3b.

The GaAsP–GaInAsSb system can have several other potential applications such as high electron mobility transistors (HEMT) and high-speed detectors. The multilayered structure is lattice-matched to the GaAs substrate and thus free from lattice defects. The HEMT can take advantage of the high mobility of the low-bandgap material in the channel and also the large band-edge discontinuity that will offer better electron confinement.

In conclusion, we have grown GaInAsSb quaternary alloy by OMCVD. We have also grown superlattice structures made of ternary–ternary and ternary–quaternary alloys. Growth conditions were adjusted to grow GaAsP–GaInAsP with a lattice parameter that is matched to the GaAs substrate, and LED's based on this SL have been demonstrated. These SL structures were disordered to obtain quaternary and quinary compounds.

Acknowledgement

This work is supported by NASA and the Army Office of Research.

References

[1] L.L. Chang, N.J. Kawai, E.E. Mendez, C.A. Chang and L. Esaki, Appl. Phys. Letters 38 (1981) 30.
[2] W.D. Laidig, J.W. Lee, P.K. Chiang, L.W. Simpson and S.M. Bedair, J. Appl. Phys. 54 (1983) 6382.

[3] I.J. Fritz, L.R. Dawson, G.C. Osbourn, P.L. Gourley and R.M. Biefeld, in: Proc. Intern. Symp. on GaAs and Related Compounds, 1982, p. 241.
[4] J.W. Matthews and A.E. Blakeslee, J. Crystal Growth 27 (1974) 118.
[5] J.P. Faurie, A. Million and J. Piaguet, Appl. Phys. Letters 34 (1979) 663.
[6] S.M. Bedair, T. Katsuyama, M. Timmons and M.A. Tischler, IEEE Electron Device Letters EDL-5 (1984) 45.
[7] M.K. Kim, M. Timmons, J.R. Hauser and S.M. Bedair, Electronic Materials Conf., Fort Collins, CO, 1982.
[8] S.M. Bedair, M.L. Timmons, P.K. Chiang, L. Simpson and J.R. Hauser, J. Electron. Mater. 12 (1983) 959.
[9] S.M. Bedair and P.K. Chiang, Electronic Materials Conf., Burlington, VT, 1983.
[10] T.H. Glisson, J.R. Hauser, M.A. Littlejohn and C.K. Williams, J. Electron. Mater. 1 (1978) 1.
[11] T. Saitoh and S. Minagawa, J. Electrochem. Soc. 120 (1973) 656.
[12] M. Armin Segmuller and A.E. Blakeslee, J. Appl. Cryst. 6 (1975) 20.
[13] S.M. Bedair et al., to be publsihed.

A New GaAsP–InGaAs Strained-Layer Superlattice Light-Emitting Diode

S. M. BEDAIR, T. KATSUYAMA, M. TIMMONS, MEMBER, IEEE, AND M. A. TISCHLER

Abstract—**The $GaAs_{1-y}P_y$-$In_xGa_{1-x}As$ superlattice (SL) system with $y = 2x$ has an average lattice constant equal to that of GaAs, thus allowing the fabrication of lattice-matched strained-layer double heterostructures. This new system can provide a large conduction band-edge discontinuity and higher electron mobility than the AlGaAs–GaAs system. The strained layers and subsequent GaAs layers epitaxially grown on them were found to be of high quality. Light-emitting diodes (LED's), based on this new superlattice, have been fabricated with emission in the wavelength range 0.9–1.1 μm. These LED's have operated for 200 h without any degradation in the output emission intensity. Also a dual-wavelength three-terminal device LED emitting near 0.87 and 0.9 μm has been fabricated. This is one of the first demonstrations of the potential applications of strained-layer superlattices (SLS).**

SUPERLATTICE (SL) structures are of both fundamental and technical interest and two classes of superlattices have been investigated. In the first class the superlattice layers have lattice parameters that closely match those of the substrate, such as in the case of the GaAs–AlGaAs and $In_{0.53}Ga_{0.47}As$–InP systems. In the second class, the strained-layer superlattice (SLS) [1], the alternating layers have lattice parameters that are different by a significant amount, but the layers are thin enough to ensure that the lattice mismatch is entirely accommodated by elastically straining the layers without the generation of misfit dislocations. Examples of these SLS are the GaAs–InGaAs [2] and GaAs–GaAsP systems [3]. These SLS have an average lattice parameter that is different from that of the substrate such as GaAs. Thus a buffer layer with the appropriate composition and lattice parameter is needed to provide lattice matching to the SLS. For example, a GaAs–$In_{0.2}Ga_{0.8}As$ SL can be grown on a GaAs substrate through an intermediate $In_{0.1}Ga_{0.9}As$ buffer layer which is not lattice matched to the GaAs substrate. This restriction may generate misfit dislocation and will not allow the use of high band-gap material such as AlGaAs as a confining or window layer for double heterostructures as needed for several optoelectronic devices. Here we present a new SLS structure made in the $GaAs_{1-y}P_y$–$In_xGa_{1-x}As$ ternary system. In such structures, with $y \approx 2x$, and with equal layer thicknesses when grown directly on a GaAs substrate, the InGaAs layers will be under compression whereas the GaAsP layers will be under tension and the lattice parameter of the SL layers will be equal to that of GaAs. Such a structure will thus allow the use of GaAs and AlGaAs as buffer layers and as confining layers, and all the layers including the SLS have the same lattice parameter. This structure can have potential applications in several electronic devices such as high electron mobility transistors, high-speed detectors, and light-emitting diodes (LED's) in the long wavelength regions. This new SLS system may have a larger conduction band-edge discontinuity than the AlGaAs–GaAs system. This would be an advantage in field-effect transistors where field strength in the channel may heat the electrons sufficiently to excite them back into the AlGaAs. It should also be noted that having the potential well for electrons in the InGaAs, one of the alloys with very high electron mobility, can lead to electron mobilities higher than those achieved in the AlGaAs–GaAs system.

We report here, as an example of the potential applications of the $GaAs_{1-y}P_y$-$In_xGa_{1-x}As$ SLS, the successful operation of double heterostructure light-emitting diodes (DH-LED) with the active layer made in the SLS. By varying the value of x and y ($y = 2x$) such an LED can operate in the wavelength range 0.87 to 1.59 μm, corresponding to $x = 0$ and $y = 1$, respectively, i.e., including the ranges where minimum absorption in optical fibers is present, thus covering a spectral range even wider than can presently be achieved by the InGaAsP/InP system. Also the emission process in SLS takes place in the low band-gap InGaAs potential well, with better carrier confinement, thus allowing a more efficient radiative recombination process.

The SLS structure has been grown by OM-CVD using TEI, TMG, AsH_3, and PH_3 as sources for the In, Ga, As, and P, respectively. The crystal growth was first calibrated with respect to compositions x and y such that $y \approx 2x$ for the $In_xGa_{1-x}As$ and $GaAs_{1-y}P_y$, respectively. The growth rate, examined on thick layers, was also calibrated to have the same thickness for the two ternary layers. A superlattice consisting of 45 layers of $L_B \sim 170$ Å of $GaAs_{0.8}P_{0.2}$ barrier alternating with 45 layers $L_Z \sim 170$ Å of $In_{0.1}Ga_{0.9}As$ quantum wells was grown on a GaAs substrate. The period ($L_Z + L_B$), of the SLS has been obtained from the X-ray diffraction pattern [4] shown in Fig. 1. The zero-order diffraction peak $n = 0$ gives the lattice parameter of the SLS, with a lattice mismatch of less than 0.1 percent to the GaAs substrate. The extra satellite peaks are due to the periodicity of the structure [4], giving $L_Z + L_B = 350$ Å, which is consistent with the value obtained from the total thickness of the SLS structures obtained on a cleaved sample. When Zn was used to disorder this SL [5], the lattice parameter of the disordered SL, which in this case is an

Manuscript received September 29, 1983; revised November 23, 1983. This work was supported by the Naval Research Laboratory and the Army Office of Research.

S. M. Bedair, T. Katsuyama, and M. A. Tischler are with North Carolina State University, Electrical and Computer Engineering Department, Raleigh, NC 27650.

M. Timmons is with the Research Triangle Institute, Research Triangle Park, NC 27709.

0193-8576/84/0200-0045$01.00

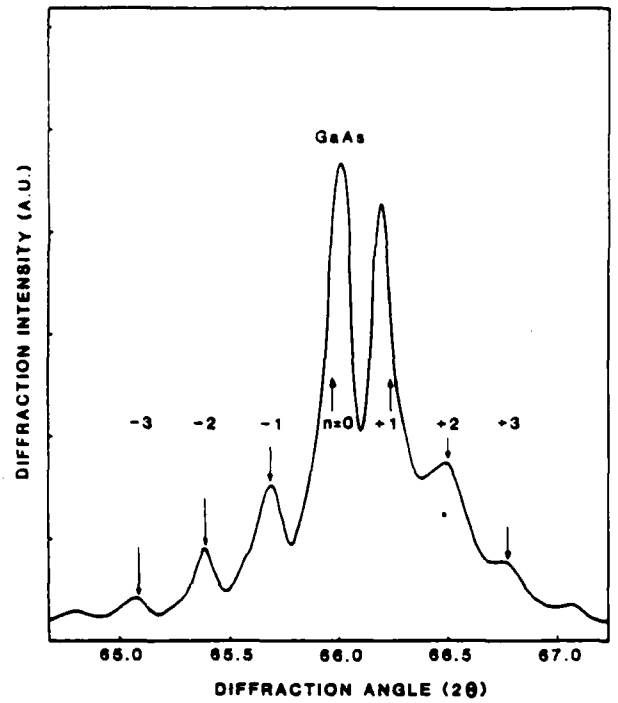

Fig. 1. X-ray diffraction pattern (400) of $GaAs_{0.8}P_{0.2}$-$In_{0.1}Ga_{0.9}As$ SLS. n's show the order of the satellite peaks originating from the periodicity of the SLS.

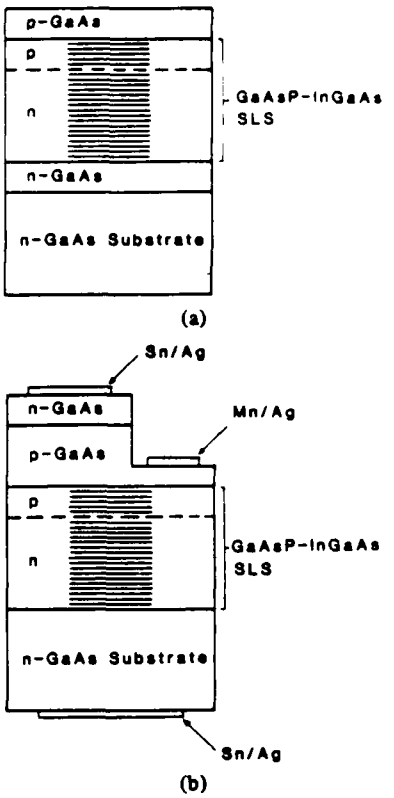

Fig. 2. Schematics of the LED structures. The $GaAs_{0.8}P_{0.2}$-$In_{0.1}Ga_{0.9}As$ SLS is made of 90 layers, ~170 Å thick each with total thickness of 1.5 μm.

InGaAsP quaternary, was found to correspond to the lattice parameter for the $n = 0$ peak shown in Fig. 1.

The surface of the GaAsP-InGaAs SLS does not have any lattice misfit dislocation network or cross-hatched structure. This is in contrast to GaAs-InGaAs SLS grown in our laboratory where a slight cross-hatched structure has always been observed. This cross-hatched structure [6] is a result of inclined dislocations that may have originated in the $In_{0.1}Ga_{0.9}As$ buffer layer which is not lattice matched to the GaAs substrate and which then propagates to the GaAs-InGaAs SLS. In order to investigate the quality of epitaxial layers grown on SLS, a thick layer of GaAs (4 μm thick) was deposited on the GaAsP-InGaAs SLS structure. Initial results indicate that etch pit counts on this GaAs epilayer are at least as low as those obtained when GaAs is grown directly on a GaAs substrate. Thus from the above observations we can conclude that the GaAsP-InGaAs SLS is grown with a lattice parameter equal to that of GaAs, thus allowing the growth of a multilayer structure without generating misfit dislocations.

An LED structure is shown in Fig. 2, where the active layer is made in the $In_{0.1}Ga_{0.9}As$-$GaAs_{0.8}P_{0.2}$ SLS. DMZ and DET have been used for p- and n-type dopants, respectively. Doping levels are in the high $10^{17}/cm^3$ range for both electrons and holes. Device fabrication uses standard metallization and etching techniques and the emission spectra are shown in Fig. 3. Lifetime tests were performed at 25°C, and several uncoated diodes were aged under constant injection levels ~20 A/cm^2 for 200 h. We have not observed any degradation in the output emission intensity for such operation time.

In order to show the advantages of having the SLS matching to GaAs, an LED was also fabricated in the GaAs-$In_{0.2}Ga_{0.8}As$ SLS with a structure similar to that shown in Fig. 2(a) but with the addition of the $In_{0.1}Ga_{0.9}As$ buffer layer [7]. As shown in Fig. 3 the emission intensity of the present lattice-matched structure is superior to that obtained in the mismatched SLS operated at the same wavelength (~1 μm) and current-injection level. A three-terminal dual-

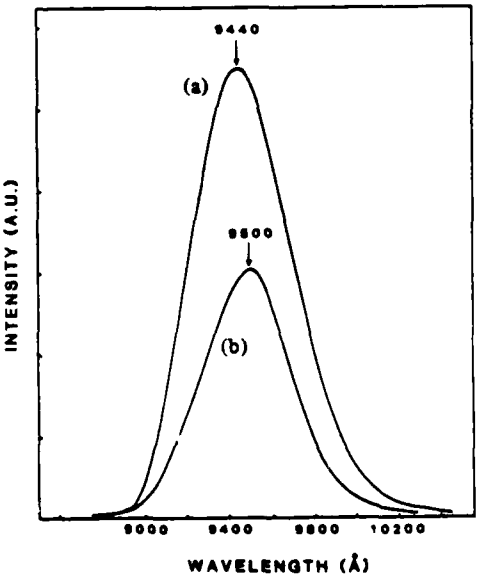

Fig. 3. Emission spectra of LED. (*a*) $GaAs_{0.8}P_{0.2}$-$In_{0.1}Ga_{0.9}As$ SLS active layer grown directly on a GaAs substrate. (*b*) GaAs-$In_{0.2}Ga_{0.9}As$ SLS active layer grown on a GaAs substrate through an intermediate $In_{0.1}Ga_{0.9}As$ buffer layer.

wavelength LED shown in Fig. 2(b), has also been fabricated. The emission spectra shows peaks at 0.9 and 0.87 μm resulting from current injection across the SLS and the GaAs junction, respectively. Initial results, from our nonoptimized structure, indicate that the GaAs LED has a lower efficiency than the SLS one, mainly due to the high series resistance. The usefulness of the SLS, grown lattice matched to GaAs, is apparent because it allows the short wavelength LED to be fabricated from material other than GaAs, such as AlGaAs or AlGaInP, and still be matched to GaAs.

In conclusion, the $GaAs_{1-y}P_y$-$In_xGa_{1-x}As$ SLS can be grown lattice-matched to GaAs substrates,thus allowing several unique device structures. LED's manufactured from this SL showed long-term stability and are superior to other SLS devices that do not lattice match to their substrates. This is one of the first demonstrations of the potential applications of SLS structures. Other SLS systems such as GaAsP-GaAsSb and GaAsP-InGaAsSb can be lattice-matched to GaAs substrates and are presently under study in our laboratory for possible device applications.

ACKNOWLEDGMENT

The authors wish to acknowledge J. R. Hauser for helpful discussions, R. Sillmon and P. K. Chiang for technical assistance, and K. Julian for the typing of this manuscript.

REFERENCES

[1] G. C. Osbourn, *J. Appl. Phys.*, vol. 53, p. 1586, 1982.
[2] W. D. Laidig, J. W. Lee, P. K. Chiang, L. W. Simpson, and S. M. Bedair, *J. Appl. Phys.*, vol. 54, p. 6382, Nov. 1983.
[3] J. W. Matthews and A. E. Blakeslee, *J. Cryst. Growth*, vol. 27, p. 118, 1974.
[4] M. Armin Segmuller and A. E. Blakeslee, *J. Appl. Cryst.*, vol. 6, p. 20, 1975.
[5] S. M. Bedair *et al.*, to be published.
[6] G. H. Olsen, C. J. Nuese, and R. T. Smith, *J. Appl. Phys.*, vol. 49, p. 5523, 1978.
[7] I. J. Fritz, L. R. Dawson, G. C. Osbourn, P. L. Gourley, and R. M. Biefeld, in *Int. Symp. GaAs and Related Compounds*, p. 241, 1982.

END

10-87

DTIC